

Accurate relativistic chiral nucleon-nucleon interaction up to NNLO

Jun-Xu Lu,^{1,2} Chun-Xuan Wang,² Yang Xiao,^{2,3} Li-Sheng Geng,^{2,4,5,*} Jie Meng,⁶ and Peter Ring⁷

¹School of Space and Environment, Beihang University, Beijing 102206, China

²School of Physics, Beihang University, Beijing 102206, China

³Université Paris-Saclay, CNRS/IN2P3, IJCLab, 91405 Orsay, France

⁴Beijing Key Laboratory of Advanced Nuclear Materials and Physics, Beihang University, Beijing 102206, China

⁵School of Physics and Microelectronics, Zhengzhou University, Zhengzhou, Henan 450001, China

⁶State Key Laboratory of Nuclear Physics and Technology,

School of Physics, Peking University, Beijing 100871, China

⁷Physik Department, Technische Universität München, D-85747 Garching, Germany

We construct a relativistic chiral nucleon-nucleon interaction up to the next-to-next-to-leading order in covariant baryon chiral perturbation theory. We show that a good description of the np phase shifts up to $T_{\text{lab}} = 200$ MeV and even higher can be achieved with a $\tilde{\chi}^2/\text{d.o.f.}$ less than 1. Both the next-to-leading order results and the next-to-next-to-leading order results describe the phase shifts equally well up to $T_{\text{lab}} = 200$ MeV, but for higher energies, the latter behaves better, showing satisfactory convergence. The relativistic chiral potential provides the most essential inputs for relativistic ab initio studies of nuclear structure and reactions, which has been in need for almost two decades.

The nucleon-nucleon (NN) interaction plays an essential role in our microscopic understanding of nuclear physics. Starting from the pioneering works of Weinberg [1–3], chiral effective field theory (ChEFT) has been successfully applied to derive the NN interaction. Nowadays the so-called chiral nuclear forces have been constructed up to the fifth order [4–6] and sixth order [7] and reached the level of the most refined phenomenological forces, such as Argonne V₁₈ [8] and CD-Bonn [9], and have become the de facto standard in ab initio nuclear structure and reaction studies [10–13].

Nonetheless, these forces are based on the non-relativistic heavy baryon chiral perturbation theory (ChPT) and cannot be used in relativistic many-body studies [14–18], for which till now only the Bonn potential [19] has been widely used [20]. In addition, there are continuing discussions on the relevance of renormalization group invariance and how the Weinberg power counting should be modified to allow for proper non-perturbative renormalization group invariance [21, 22]. Lorentz covariance, as one of the most fundamental requirements of Nature, may play a role here. It is particularly inspiring to note that in the one-baryon sector covariant baryon ChPT has been shown to provide new perspectives on a number of long standing puzzles, such as baryon magnetic moments [23], Compton scattering off protons [24], pion-nucleon scattering [25], and baryon masses [26, 27]. See Ref. [28] for a short review.

Recently, a covariant power counting approach similar to the extended-on-mass-shell scheme in the one-baryon sector [29, 30] was proposed to describe the NN interaction [31, 32].¹ At leading order (LO), the covariant scheme has been successfully tested in the NN system [31, 37–40], hyperon-nucleon system [41–46], and $\Lambda_c N$ system [47, 48].

In addition to providing already a reasonable description of the $J = 0, 1$ np phase shifts at LO, it also shows some interesting features of proper effective field theories. In Ref. [37], it was shown that for the 1S_0 partial wave, some of the typical low energy features can be reproduced at LO, contrary to the conventional Weinberg approach. In addition, it also shows improved renormalization group invariance, for example, in the 3P_0 channel [40]. In Ref. [49], it was shown in a hybrid phenomenological approach that the LO relativistic three-body interaction leads to a satisfactory description of polarized pd scattering data in the whole energy range below the deuteron breakup threshold, solving the longstanding A_y puzzle thanks to the new terms considered in the $3N$ force. Furthermore, in Ref. [50], it was shown that the relativistic effects in the perturbative two-pion-exchange (TPE) contributions do improve the description of the peripheral NN scattering data compared to their non-relativistic counterparts. In Ref. [51], the same feature is found also for the non-perturbative TPE contributions.

Nonetheless, for realistic studies of nuclear structure and reactions, the relativistic chiral force has to be constructed to higher chiral orders. Furthermore, a complete understanding of the relativistic chiral nuclear force beyond leading order is also of high relevance. For such purposes, in the present work, we construct the first accurate relativistic NN interaction up to the next-to-next-to-leading order (NNLO).²

In order to take into account the non-perturbative nature of the NN interaction, we solve the following relativistic Blankenbecler-Sugar (BbS) equation [53],

$$T(\mathbf{p}', \mathbf{p}, s) = V(\mathbf{p}', \mathbf{p}, s) + \int \frac{d^3k}{(2\pi)^3} V(\mathbf{p}', \mathbf{k}, s) \frac{m^2}{E_k} \frac{1}{\mathbf{q}_{cm}^2 - \mathbf{k}^2 - i\epsilon} T(\mathbf{k}, \mathbf{p}, s), \quad (1)$$

¹ We note that a modified Weinberg's approach to the NN scattering problem was proposed in Ref. [33], which employs time-ordered perturbation theory and relies on the manifestly Lorentz-invariant effective Lagrangian and aims at improving the UV behavior of Weinberg's approach [34–36].

² Recent studies show that the NNLO non-relativistic chiral forces can provide reliable inputs already, but the N³LO forces yield smaller uncertainties [52].

where $|q_{cm}| = \sqrt{s/4 - m^2}$ is the nucleon momentum on the mass shell in the center of mass (c.m.) frame, and a sharp cutoff Λ is introduced to regularize the potential and its value will be specified later. The momenta of the incoming, outgoing, and intermediate nucleons are depicted in Fig. 1, consistent with the 3D reduction of the Bethe-Salpeter equation to the BbS equation [54].

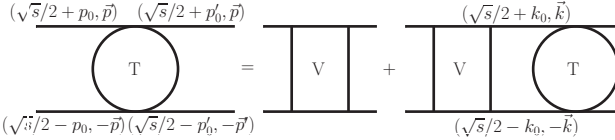


FIG. 1. Relativistic kinematics of nucleon-nucleon scattering.

Up to NNLO, the relativistic chiral potential consists of the following terms

$$V = V_{CT}^{\text{LO}} + V_{CT}^{\text{NLO}} + V_{\text{OPE}} + V_{\text{TPE}}^{\text{NLO}} + V_{\text{TPE}}^{\text{NNLO}} - V_{\text{IOPE}}, \quad (2)$$

in which the first two terms refer to the LO [$\mathcal{O}(p^0)$] and NLO [$\mathcal{O}(p^2)$] contact contributions, while the next three terms denote the one-pion exchange (OPE), leading, and subleading TPE contributions. The last term represents the iterated OPE contribution.

The chiral effective Lagrangians for the nucleon-nucleon interaction in covariant baryon ChPT have been constructed up to $\mathcal{O}(p^4)$ in Ref. [32]. There are four contact terms at LO, 13 terms at NLO, and no contact terms at NNLO. As is argued in the Supplementary Material, the large subleading TPE contributions affect the descriptions of some higher partial waves, especially 3P_2 . Relevant discussions in the non-relativistic cases can be found in Refs. [55–57]. In order to partially compensate the large subleading TPE contributions to the 3P_2 channel, we promote two nominal N³LO contact terms to NLO. Considering that in our covariant power counting, the NLO contact terms already contain terms of $\mathcal{O}(p^4)$ as is depicted in the Supplementary Material, we promote the same terms but originally counted as of N³LO to NLO for the 3P_2 - 3F_2 partial waves. This is equivalent to removing part of the correlations between the higher order contact terms for 3P_2 - 3F_2 and the other $J = 2$ partial waves. Therefore, in the end, we have in total 19 low-energy constants (LECs) up to NNLO. We note that although this number is larger than that of the non-relativistic NNLO potential (9) but smaller than that of N³LO (24) [57, 58]³. In our relativistic framework, the 19 LECs contribute to all the partial waves with total angular momentum $J \leq 2$, which makes it impossible to reorganize the LECs according to partial waves, different from the non-relativistic cases⁴. We refer to the Supplementary Ma-

terial for the explicit expressions of the LO and NLO contact potentials.

For the treatment of non-perturbative OPE and TPE contributions, we refer to Ref. [51]. In Table I, we show the values of LECs needed to evaluate the OPE and TPE contributions.

TABLE I. Decay constant f_π (in units of MeV) [11], coupling constant g_A [11], and NLO πN couplings (in units of GeV^{-1}) [59] adopted for evaluating the OPE and TPE diagrams.

| c_1 | c_2 | c_3 | c_4 | f_π | g_A |
|-------|-------|-------|-------|---------|-------|
| -1.39 | 4.01 | -6.61 | 3.92 | 92.4 | 1.29 |

An important feature of ChEFT is that it allows for reliable uncertainty quantification. In the literature, two different ways have been used to estimate the truncation uncertainties of chiral nuclear forces. One is varying the cutoff in a reasonable range, for example, from 450 MeV to 550 MeV [11]. The other is to treat the difference between the optimal results obtained at different orders as the estimate of truncation uncertainties [4]. Recently, a general Bayesian model has been proposed [60–62] and applied in the latest non-relativistic studies [63–65], which we follow in the present work. This method is statistically well-established and can provide a statistical interpretation for the estimated uncertainties. For a detailed account of the implementation of this approach in the present study, see the Supplementary Material.

In Ref. [51], we showed that the higher partial waves which do not receive contact contributions up to NNLO can be well described with a cutoff of 0.9 GeV. In addition, only the 3D_3 partial wave is sensitive to the cutoff, which implies that higher order LECs are needed for this particular partial wave to achieve renormalization group invariance. As a result, in the fitting of the LECs at NLO and NNLO, we fix the cutoff at 0.9 GeV.

Following the strategy adopted in non-relativistic studies, e.g., Refs. [4, 68], we perform a global fit to the np phase shifts for all the partial waves with total angular momentum $J \leq 2$ [67].⁵ For each partial wave, we choose eight data points with laboratory kinetic energy $T_{\text{lab}} = 1, 5, 10, 25, 50, 100, 150, 200$ MeV for the fitting. The χ^2 -like function to be minimized, $\tilde{\chi}^2$, is defined as

$$\tilde{\chi}^2 = \sum_i (\delta^i - \delta_{\text{PWA93}}^i)^2, \quad (3)$$

where δ^i are theoretical phase shifts or mixing angles, and δ_{PWA93}^i are their empirical PWA93 counterparts [67]. A few remarks are in order. First, the $\tilde{\chi}^2$ defined above does not have proper statistic meaning, as no uncertainties are assigned and the number of data fitted is a bit arbitrary (eight for each

³ It should be noted that the two isospin-violating LECs are not included here. Furthermore, the results of Ref. [58] with which we compare were obtained by setting $c_{2,3,4}$ semi-free.

⁴ Note that in the non-relativistic framework, there is no LEC for the 3F_2 partial wave up to N³LO.

⁵ For a justification of direct fits to phase shifts, see, Ref. [69]. An alternative fit to the results of the Granada partial wave analysis [70–72] is given in the Supplementary Material.

TABLE II. LECs (in units of 10^4 GeV^{-2}) for the relativistic LO, NLO, and NNLO results shown in Fig. 2.

| | O_1 | O_2 | O_3 | O_4 | O_5 | O_6 | O_7 | O_8 | O_9 | O_{10} | O_{11} | O_{12} | O_{13} | O_{14} | O_{15} | O_{16} | O_{17} | D_1 | D_2 |
|------|--------|-------|-------|-------|-------|-------|-------|-------|-------|----------|----------|----------|----------|----------|----------|----------|----------|-------|-------|
| LO | -1.32 | -0.21 | -0.93 | 0.31 | | | | | | | | | | | | | | | |
| NLO | -2.62 | 9.45 | -5.42 | -6.05 | 30.09 | 9.02 | -9.19 | 8.74 | 4.74 | 7.02 | 3.52 | 11.42 | -6.03 | -20.55 | -4.99 | -12.80 | 6.30 | 0.42 | 0.28 |
| NNLO | -14.83 | -2.25 | -4.85 | 6.24 | -0.82 | 1.96 | -6.89 | 7.19 | 1.44 | 3.50 | -8.10 | -9.38 | -4.33 | -12.89 | -12.26 | -11.69 | 3.86 | -1.88 | -0.63 |

TABLE III. $\tilde{\chi}^2 = \sum_i (\delta^i - \delta_{\text{PWA93}}^i)^2$ of different chiral forces for partial waves up to $J \leq 2$.

| | Total | 1S_0 | 3P_0 | 1P_1 | 3P_1 | 3S_1 | 3D_1 | ϵ_1 | 1D_2 | 3D_2 | 3P_2 | 3F_2 | ϵ_2 |
|----------------------------|-------|-----------|-----------|-----------|-----------|-----------|-----------|--------------|-----------|-----------|-----------|-----------|--------------|
| NLO | 17.02 | 1.02 | 7.04 | 0.46 | 0.33 | 1.80 | 1.69 | 0.15 | 2.18 | 1.35 | 0.95 | 0.01 | 0.04 |
| NNLO | 16.61 | 0.18 | 0.30 | 1.07 | 1.55 | 3.36 | 0.26 | 0.03 | 0.01 | 9.56 | 0.01 | 0.27 | 0.01 |
| NR-N ³ LO-Idaho | 8.84 | 1.53 | 0.30 | 2.41 | 0.04 | 2.33 | 1.00 | 0.02 | 0.57 | 0.42 | 0.17 | 0.03 | 0.02 |
| NR-N ³ LO-EKM | 16.08 | 13.45 | 0.29 | 0.34 | 0.06 | 0.01 | 0.13 | 0.01 | 0.02 | 0.43 | 0.12 | 1.22 | 0.00 |

partial wave in the present study). Second, as the same uncertainties for the phase shifts and mixing angle are assumed, this necessarily put more weights on those partial waves of large magnitude, for example, 1S_0 and 3S_1 .

The so-obtained fitting results are shown in Fig. 2, where the theoretical uncertainties are obtained via the Bayesian model explained in the Supplementary Material for a DoB level of 68%. The corresponding LECs are given in Table II. For comparison, we also show the non-relativistic N³LO results obtained with different strategies for regularizing chiral potentials from Refs. [11, 58] and Refs. [4, 66] which are denoted as NR-N³LO-Idaho and NR-N³LO-EKM, respectively. Comparing the LO, NLO, and NNLO results as well as the uncertainties, it is clear that the chiral results are converging reasonably well. In addition, the LECs look quite natural, particularly, those at NNLO, as the magnitude of most of them is in between 1 ~ 10, though O_1 , O_{14} , O_{15} , and O_{16} are perhaps a little bit large, but not abnormally large.

First we notice that the NLO and NNLO relativistic results describe the np phase shifts very well up to $T_{\text{lab}} = 200$ MeV, at a level similar to the non-relativistic N³LO results. Particularly interesting is that the NLO and the NNLO results also agree well with each other for $T_{\text{lab}} \leq 200$ MeV, while the NNLO results are in better agreement the PWA93 data for larger kinetic energies. This demonstrates that the chiral series converge well. On the other hand, for 3F_2 , the NLO results are better, which can be attributed to the compromise that one has to make to fit all the $J = 2$ partial waves with five LECs to balance the large contributions of subleading TPE. It can be largely improved once the correlation between the D -waves with $J = 2$ and 3P_2 - 3F_2 are removed, i.e., the D -waves and 3P_2 - 3F_2 are fitted separately or the cutoff is slightly modified. We note that in obtaining the NR-N³LO-Idaho results, the phase shifts of this channel were lowered by a careful fine-tuning of c_2 and c_4 [58].

The $\tilde{\chi}^2$'s for each partial wave are given in Table III. Judging from the total $\tilde{\chi}^2$, the quality of the relativistic fits is compatible to the non-relativistic N³LO results. Comparing the NR-N³LO-EKM results with the relativistic NNLO results,

we find that although the total $\tilde{\chi}^2$'s are similar, they originate from different partial waves. The largest contribution to the total $\tilde{\chi}^2$ of NR-N³LO-EKM comes from the 1S_0 partial wave while that of our NNLO results originates from the 3D_2 partial wave. It should also be noted that if we set the cutoff at 0.8 GeV, we can achieve a total $\tilde{\chi}^2$ as small as 5.3 (see the Supplementary Material for details), which is even smaller than that of NR-N³LO-Idaho, which is about 9. However, as shown in Ref. [51], the 3D_3 partial wave cannot be well described with a cutoff of 0.8 GeV. Therefore, in the present work, we stick to the cutoff of 0.9 GeV.⁶

To summarize, we constructed a relativistic chiral nucleon-nucleon interaction up to the next-to-next-to-leading order in covariant baryon chiral perturbation theory. The 19 low energy constants were fixed by fitting to all the partial wave phase shifts with total angular momentum $J \leq 2$. We obtained a good description of the PWA93 phase shifts. The next-to-leading order and the next-to-next-to-leading order results agree well with each other for $T_{\text{lab}} \leq 200$ MeV, while at higher energies the NNLO results agree better with the PWA93 phase shifts. This demonstrated the convergence of the covariant chiral expansions. Given the quality already achieved in describing the np phase shifts, the NNLO relativistic chiral NN interaction provides the much wanted inputs for relativistic ab initio nuclear structure and reaction studies. In particular, it may provide new insights into many long-standing problems, e.g., the A_y puzzle, in combination with the leading order relativistic $3N$ chiral force explored in Ref. [49], which appears at NNLO.

⁶ It should be mentioned that the relatively large cutoff together with the pion-nucleon couplings c_i determined from pion-nucleon scattering (which result in strongly attractive subleading TPE contributions in some channels) could lead to the appearance of deeply bound states (see Ref. [5] for a detailed discussion). Although they are beyond the range of the EFT and are irrelevant for the low-energy physics [68, 73], they could potentially complicate many-body calculations (See Ref. [73] for a solution). We leave a study of their impact on relativistic ab initio calculations to a future work.

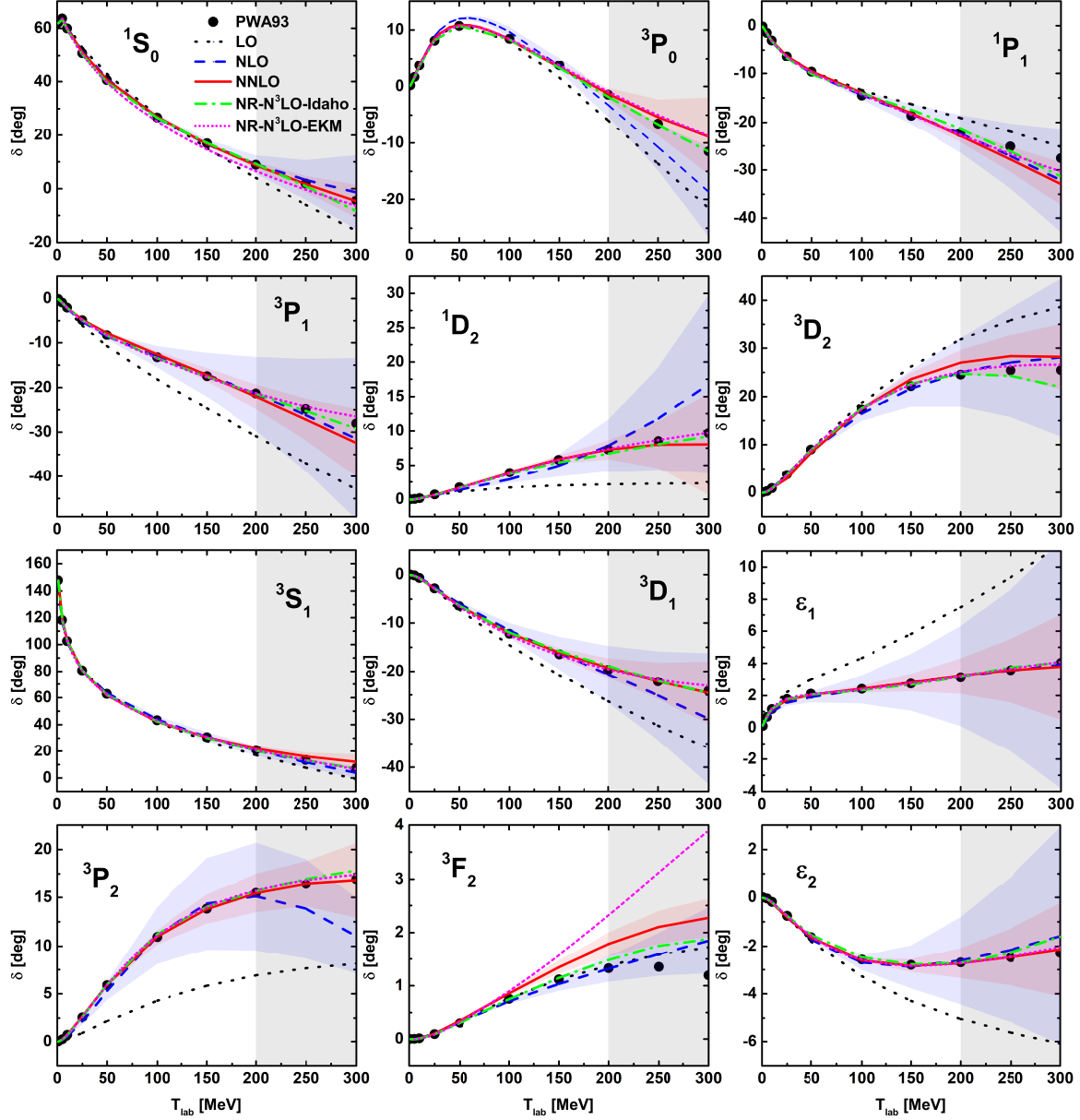


FIG. 2. NN phase shifts for partial waves with $J \leq 2$. The red solid lines denote the relativistic NNLO results obtained with a cutoff of $\Lambda = 0.9$ GeV and the blue dashed lines denote the relativistic NLO results obtained with a smaller cutoff of $\Lambda = 0.6$ GeV. The corresponding bands represent the uncertainties for a DoB level of 68%. For comparison, we also show the LO relativistic results (black dotted lines) obtained with a cutoff of $\Lambda = 0.6$ GeV and the two sets of non-relativistic N^3LO results NR- N^3LO -Idaho ($\Lambda = 0.5$ GeV, green dash-dotted lines) [11, 58] and NR- N^3LO -EKM (cutoff = 0.9 fm, magenta short-dotted lines) [4, 66]. The black dots denote the PWA93 phase shifts [67]. The shaded regions denote that those data are not fitted and the corresponding relativistic results are predictions.

This work is supported in part by the National Natural Science Foundation of China under Grants No.11735003, No.11975041, and No.11961141004. Jun-Xu Lu acknowledges support from the National Natural Science Foundation of China under Grants No.12105006. Jie Meng acknowledges support from the National Science Foundation of China (NSFC) under Grants No. 11935003 and the National Key R & D Program of China (Contracts

No. 2017YFE0116700). Peter Ring acknowledges partial support from the Deutsche Forschungsgemeinschaft (DFG, German Research Foundation) under Germany's Excellence Strategy—EXC-2094—390783311.

* Corresponding author: lisheng.geng@buaa.edu.cn

- [1] S. Weinberg, Phys. Lett. **B251**, 288 (1990).
- [2] S. Weinberg, Nucl. Phys. **B363**, 3 (1991).
- [3] S. Weinberg, Phys. Lett. B **295**, 114 (1992), arXiv:hep-ph/9209257.
- [4] E. Epelbaum, H. Krebs, and U.-G. Meißner, Phys. Rev. Lett. **115**, 122301 (2015).
- [5] P. Reinert, H. Krebs, and E. Epelbaum, Eur. Phys. J. A **54**, 86 (2018), arXiv:1711.08821 [nucl-th].
- [6] D. R. Entem, R. Machleidt, and Y. Nosyk, Phys. Rev. C **96**, 024004 (2017).
- [7] D. Rodriguez Entem, R. Machleidt, and Y. Nosyk, Front. in Phys. **8**, 57 (2020).
- [8] R. B. Wiringa, V. G. J. Stoks, and R. Schiavilla, Phys. Rev. C **51**, 38 (1995).
- [9] R. Machleidt, Phys. Rev. C **63**, 024001 (2001).
- [10] E. Epelbaum, H.-W. Hammer, and U.-G. Meißner, Rev. Mod. Phys. **81**, 1773 (2009).
- [11] R. Machleidt and D. R. Entem, Phys. Rept. **503**, 1 (2011).
- [12] H. W. Hammer, S. König, and U. van Kolck, Rev. Mod. Phys. **92**, 025004 (2020), arXiv:1906.12122 [nucl-th].
- [13] C. Drischler, W. Haxton, K. McElvain, E. Mereghetti, A. Nicholson, P. Vranas, and A. Walker-Loud, Prog. Part. Nucl. Phys. **121**, 103888 (2021), arXiv:1910.07961 [nucl-th].
- [14] S. Shen, J. Hu, H. Liang, J. Meng, P. Ring, and S. Zhang, Chin. Phys. Lett. **33**, 102103 (2016).
- [15] S. Shen, H. Liang, J. Meng, P. Ring, and S. Zhang, Phys. Rev. C **96**, 014316 (2017), arXiv:1705.01691 [nucl-th].
- [16] H. Tong, X.-L. Ren, P. Ring, S.-H. Shen, S.-B. Wang, and J. Meng, Phys. Rev. C **98**, 054302 (2018), arXiv:1808.09138 [nucl-th].
- [17] H. Tong, P.-W. Zhao, and J. Meng, Phys. Rev. C **101**, 035802 (2020), arXiv:1903.05938 [nucl-th].
- [18] S. Wang, Q. Zhao, P. Ring, and J. Meng, Phys. Rev. C **103**, 054319 (2021), arXiv:2103.12960 [nucl-th].
- [19] R. Machleidt, K. Holinde, and C. Elster, Phys. Rept. **149**, 1 (1987).
- [20] S. Shen, H. Liang, W. H. Long, J. Meng, and P. Ring, Prog. Part. Nucl. Phys. **109**, 103713 (2019), arXiv:1904.04977 [nucl-th].
- [21] E. Epelbaum, A. M. Gasparyan, J. Gegelia, and U.-G. Meißner, Eur. Phys. J. A **54**, 186 (2018), arXiv:1810.02646 [nucl-th].
- [22] U. van Kolck, Front. in Phys. **8**, 79 (2020), arXiv:2003.06721 [nucl-th].
- [23] L. S. Geng, J. Martin Camalich, L. Alvarez-Ruso, and M. J. Vicente Vacas, Phys. Rev. Lett. **101**, 222002 (2008), arXiv:0805.1419 [hep-ph].
- [24] V. Lensky and V. Pascalutsa, Eur. Phys. J. C **65**, 195 (2010), arXiv:0907.0451 [hep-ph].
- [25] J. M. Alarcon, J. Martin Camalich, and J. A. Oller, Phys. Rev. D **85**, 051503 (2012), arXiv:1110.3797 [hep-ph].
- [26] J. Martin Camalich, L. S. Geng, and M. J. Vicente Vacas, Phys. Rev. D **82**, 074504 (2010), arXiv:1003.1929 [hep-lat].
- [27] X.-L. Ren, L.-S. Geng, J. Martin Camalich, J. Meng, and H. Toki, JHEP **12**, 073 (2012).
- [28] L.-S. Geng, Front. Phys.(Beijing) **8**, 328 (2013).
- [29] J. Gegelia and G. Japaridze, Phys. Rev. D **60**, 114038 (1999), arXiv:hep-ph/9908377.
- [30] T. Fuchs, J. Gegelia, G. Japaridze, and S. Scherer, Phys. Rev. D **68**, 056005 (2003), arXiv:hep-ph/0302117.
- [31] X.-L. Ren, K.-W. Li, L.-S. Geng, B.-W. Long, P. Ring, and J. Meng, Chin. Phys. C **42**, 014103 (2018).
- [32] Y. Xiao, L.-S. Geng, and X.-L. Ren, Phys. Rev. C **99**, 024004 (2019), arXiv:1812.03005 [nucl-th].
- [33] E. Epelbaum and J. Gegelia, Phys. Lett. B **716**, 338 (2012).
- [34] E. Epelbaum, A. M. Gasparyan, J. Gegelia, and H. Krebs, Eur. Phys. J. A **51**, 71 (2015).
- [35] J. Behrendt, E. Epelbaum, J. Gegelia, U.-G. Meißner, and A. Nogga, Eur. Phys. J. A **52**, 296 (2016).
- [36] X.-L. Ren, E. Epelbaum, and J. Gegelia, (2022), arXiv:2202.04018 [nucl-th].
- [37] X.-L. Ren, C.-X. Wang, K.-W. Li, L.-S. Geng, and J. Meng, Chin. Phys. Lett. **38**, 062101 (2021), arXiv:1712.10083 [nucl-th].
- [38] Q.-Q. Bai, C.-X. Wang, Y. Xiao, and L.-S. Geng, Phys. Lett. B, 135745 (2020), arXiv:2007.01638 [nucl-th].
- [39] Q.-Q. Bai, C.-X. Wang, Y. Xiao, and L.-S. Geng, (2021), arXiv:2105.06113 [hep-ph].
- [40] C.-X. Wang, L.-S. Geng, and B. Long, Chin. Phys. C **45**, 054101 (2021), arXiv:2001.08483 [nucl-th].
- [41] K.-W. Li, X.-L. Ren, L.-S. Geng, and B. Long, Phys. Rev. D **94**, 014029 (2016).
- [42] K.-W. Li, X.-L. Ren, L.-S. Geng, and B.-W. Long, Chin. Phys. C **42**, 014105 (2018), arXiv:1612.08482 [nucl-th].
- [43] K.-W. Li, T. Hyodo, and L.-S. Geng, Phys. Rev. C **98**, 065203 (2018), arXiv:1809.03199 [nucl-th].
- [44] J. Song, K.-W. Li, and L.-S. Geng, Phys. Rev. C **97**, 065201 (2018), arXiv:1802.04433 [nucl-th].
- [45] Z.-W. Liu, J. Song, K.-W. Li, and L.-S. Geng, Phys. Rev. C **103**, 025201 (2021), arXiv:2011.05510 [nucl-th].
- [46] J. Song, Z.-W. Liu, K.-W. Li, and L.-S. Geng, (2021), arXiv:2107.04742 [nucl-th].
- [47] J. Song, Y. Xiao, Z.-W. Liu, C.-X. Wang, K.-W. Li, and L.-S. Geng, Phys. Rev. C **102**, 065208 (2020), arXiv:2010.06916 [nucl-th].
- [48] J. Song, Y. Xiao, Z.-W. Liu, K.-W. Li, and L.-S. Geng, (2021), arXiv:2104.02380 [hep-ph].
- [49] L. Girlanda, A. Kievsky, M. Viviani, and L. E. Marcucci, Phys. Rev. C **99**, 054003 (2019), arXiv:1811.09398 [nucl-th].
- [50] Y. Xiao, C.-X. Wang, J.-X. Lu, and L.-S. Geng, Phys. Rev. C **102**, 054001 (2020), arXiv:2007.13675 [nucl-th].
- [51] C.-X. Wang, J.-X. Lu, Y. Xiao, and L.-S. Geng, Phys. Rev. C **105**, 014003 (2022), arXiv:2110.05278 [nucl-th].
- [52] T. Hüther, K. Vobig, K. Hebeler, R. Machleidt, and R. Roth, Phys. Lett. B **808**, 135651 (2020), arXiv:1911.04955 [nucl-th].
- [53] R. Blankenbecler and R. Sugar, Phys. Rev. **142**, 1051 (1966).
- [54] R. M. Woloshyn and A. D. Jackson, Nucl. Phys. B **64**, 269 (1973).
- [55] E. Epelbaum, W. Gloeckle, and U.-G. Meißner, Eur. Phys. J. A **19**, 125 (2004), arXiv:nucl-th/0304037.
- [56] E. Epelbaum, W. Gloeckle, and U.-G. Meißner, Eur. Phys. J. A **19**, 401 (2004), arXiv:nucl-th/0308010.
- [57] E. Epelbaum, W. Glockle, and U.-G. Meißner, Nucl. Phys. A **747**, 362 (2005).
- [58] D. R. Entem and R. Machleidt, Phys. Rev. C **68**, 041001 (2003).
- [59] Y.-H. Chen, D.-L. Yao, and H. Q. Zheng, Phys. Rev. D **87**, 054019 (2013), arXiv:1212.1893 [hep-ph].
- [60] R. J. Furnstahl, N. Klco, D. R. Phillips, and S. Wesolowski, Phys. Rev. C **92**, 024005 (2015), arXiv:1506.01343 [nucl-th].
- [61] J. A. Melendez, S. Wesolowski, and R. J. Furnstahl, Phys. Rev. C **96**, 024003 (2017), arXiv:1704.03308 [nucl-th].
- [62] J. A. Melendez, R. J. Furnstahl, D. R. Phillips, M. T. Pratola, and S. Wesolowski, Phys. Rev. C **100**, 044001 (2019), arXiv:1904.10581 [nucl-th].
- [63] E. Epelbaum et al., Eur. Phys. J. A **56**, 92 (2020), arXiv:1907.03608 [nucl-th].
- [64] E. Epelbaum, H. Krebs, and P. Reinert, Front. in Phys. **8**, 98 (2020), arXiv:1911.11875 [nucl-th].
- [65] P. Maris et al., Phys. Rev. C **103**, 054001 (2021),

- arXiv:2012.12396 [nucl-th].
- [66] E. Epelbaum, H. Krebs, and U. G. Meißner, Eur. Phys. J. **A51**, 53 (2015).
 - [67] V. G. J. Stoks, R. A. M. Klomp, M. C. M. Rentmeester, and J. J. de Swart, Phys. Rev. **C48**, 792 (1993).
 - [68] E. Epelbaum, W. Gloeckle, and U.-G. Meißner, Nucl. Phys. **A671**, 295 (2000).
 - [69] A. G. Escalante, R. Navarro Pérez, and E. Ruiz Arriola, Phys. Rev. C **104**, 054002 (2021), arXiv:2010.03885 [nucl-th].
 - [70] R. Navarro Pérez, J. E. Amaro, and E. Ruiz Arriola, Phys. Rev. C **88**, 024002 (2013), [Erratum: Phys. Rev. C 88, 069902 (2013)], arXiv:1304.0895 [nucl-th].
 - [71] R. Navarro Pérez, J. E. Amaro, and E. Ruiz Arriola, Phys. Rev. C **91**, 054002 (2015), arXiv:1411.1212 [nucl-th].
 - [72] R. Navarro Pérez, J. E. Amaro, and E. Ruiz Arriola, Phys. Rev. C **95**, 064001 (2017), arXiv:1606.00592 [nucl-th].
 - [73] A. Nogga, R. G. E. Timmermans, and U. van Kolck, Phys. Rev. C **72**, 054006 (2005).

Supplementary Material for “Accurate relativistic chiral nucleon-nucleon interaction up to NNLO”

In this supplemental material, we provide further details that are useful to understand the results presented in the main text.

FITS WITH 17 LECs

In this section, we present the NN scattering phase shifts obtained in our NNLO chiral nuclear force with 17 LECs as dictated in Ref. [1], and explain why two nominal N³LO contact terms need to be promoted.

Following the same fitting strategy as detailed in the main text, we obtain the results shown in Fig. 1. For comparison, we also show the non-relativistic NNLO and N³LO results which are referred to as “NR-NNLO” [2], “NR-N³LO-Idaho” [3, 4], and “NR-N³LO-EKM” [5, 6], respectively. In Table I, we tabulate the $\tilde{\chi}^2$ obtained by fitting to the PWA93 phase shifts at laboratory energies $T_{\text{lab}} = 1, 5, 10, 25, 50, 100, 150, 200$ MeV for each partial wave, as well as the sum of them. Clearly, compared to the results shown in the main text, only the 3P_2 partial wave cannot be satisfactorily described.

It was already noticed in Ref. [2] that the non-relativistic subleading TPE potential is a bit strong such that the description of the phase shifts can be worsened at NNLO for some partial waves, e.g., the 3P_2 partial wave. This was attributed to the dimensional regularization applied in regularizing the TPE loop diagrams that takes into account the high-momentum contribution of pion loops. Replacing the dimensional regularization with the so-called spectrum functional regularization, which is essentially a cutoff regularization, improves the description of 3P_2 at NNLO (but worsens the description of some other partial waves [7–9]). On the other hand, a better description with the dimensional regularization can be obtained when the non-relativistic chiral potential was constructed up to N³LO [3], which yields results in good agreement with the PWA93 phase shifts for all the partial waves considered there (but with a dedicated fine-tuning of the NLO πN LECs c_2 and c_4). In Refs. [5, 10], the authors presented another high-quality non-relativistic chiral potential with NLO πN LECs c_i ’s fixed using an appropriate regularization in coordinate space. In addition, since there is no LEC to balance the large TPE contributions except the cutoff and the NLO LECs of πN scattering c_1, c_2, c_3, c_4 , $V_{\text{TPE}}^{\text{NNLO}}$ introduces strong cutoff dependence for the partial waves with orbital angular momentum $L = 2$, particularly, 3D_3 . This problem can be alleviated after the non-relativistic chiral potential is constructed up to N³LO in which new LECs are introduced.

In our study, we find that the relativistic potential also suffers from the two problems mentioned above but to a less extent. The contributions from the relativistic $V_{\text{TPE}}^{\text{NNLO}}$ is large and compatible with (but smaller than) their corresponding

non-relativistic counterparts [11].

The large subleading TPE contributions force the 3P_2 phase shifts to drop down with increasing T_{lab} . To compensate them, we promote two of the higher order contact terms to NLO for the 3P_2 - 3F_2 coupled channel, which is equivalent to breaking the correlations between the $J = 2$ partial waves. In the following we explain in detail how we achieved this.

In our covariant power counting scheme [1], the NLO contact terms for the $J = 2$ partial waves already contain nominally higher order contact terms (in the language of HBChPT) as is explicitly exhibited in Eq. (22). Obviously, for the two D -waves, at this order, the contact terms are counted nominally as of $\mathcal{O}(p^4)$. For 3P_2 , the first term is counted as of order $\mathcal{O}(p^2)$, while the other two terms are of order $\mathcal{O}(p^4)$ and $\mathcal{O}(p^6)$, respectively. The situation is similar for 3F_2 and the off-diagonal 3P_2 - 3F_2 . This way, we have in total eight different structures, corresponding to eight combinations of the NLO LECs ($O_{5,\dots,17}$) for all the $J = 2$ partial waves, while only three of them are independent.

On the other hand, at N³LO, the contact terms contain the same structures of nominal order $\mathcal{O}(p^4)$ for these partial waves. The only difference is that at N³LO, the coefficients for these terms are composed of the N³LO LECs ($O_{18,\dots,40}$) [1]. The relevant terms of order $\mathcal{O}(p^4)$ for 3P_2 and 3P_2 - 3F_2 at N³LO read

$$\begin{aligned} V_{3P_2}^{N^3LO} &= D_1 \frac{\pi pp'(\Delta_p + \Delta_{p'})}{m^3}, \\ V_{3P_2-3F_2}^{N^3LO} &= D_2 \frac{\pi pp'^3}{m^3 N_p}, \end{aligned} \quad (1)$$

in which $\Delta_p, \Delta_{p'}, N_p$ are defined in Eq. (11). The D_1 and D_2 are

$$\begin{aligned} D_1 &= (-2O_{18} - O_{19} - O_{20} - 10O_{21} - 9O_{22} - 10O_{24} \\ &\quad - 10O_{25} + 10O_{26} - 20O_{27} - 2O_{28} - O_{29} - O_{30} \\ &\quad - 10O_{31} - 9O_{32} - 10O_{33} - 12O_{34} + 12O_{35} - 16O_{36} \\ &\quad - 10O_{37} - 14O_{38} + 14O_{39} - 12O_{40})/30, \\ D_2 &= -5\sqrt{\frac{3}{2}}(2O_{18} + O_{19} + O_{20} - O_{22} + 2O_{28} \\ &\quad + O_{29} + O_{30} - O_{32} + 2O_{34} - 2O_{35} - 4O_{36} + 4O_{38} \\ &\quad - 4O_{39} - 8O_{40}). \end{aligned} \quad (2)$$

In the present work, we promote these two additional terms of Eq. (1) from N³LO to $V_{3P_2}^{NLO}$ and $V_{3P_2-3F_2}^{NLO}$ in Eq. (22). This is equivalent to performing the following replacements,

$$C_2^{3P2} \rightarrow C_2^{3P2} + D_1, \quad C_1^{3PF2} \rightarrow C_1^{3PF2} + D_2. \quad (3)$$

This way, we break the correlation between C_2^{3P2}, C_1^{3PF2} , and the other six combinations. We have now five independent

TABLE I. $\chi^2 = \sum_i (\delta^i - \delta_{\text{PWA93}}^i)^2$ of different chiral forces of partial waves up to $J \leq 2$.

| | Total | 1S_0 | 3P_0 | 1P_1 | 3P_1 | 3S_1 | 3D_1 | ϵ_1 | 1D_2 | 3D_2 | 3P_2 | 3F_2 | ϵ_2 |
|----------------------------|--------|---------|---------|---------|---------|---------|---------|--------------|---------|---------|---------|---------|--------------|
| NNLO | 51.64 | 0.29 | 0.29 | 1.13 | 1.50 | 3.40 | 0.01 | 0.15 | 0.01 | 9.71 | 34.73 | 0.41 | 0.03 |
| NR-NNLO | 289.59 | 2.68 | 27.49 | 2.32 | 20.96 | 0.62 | 0.25 | 1.55 | 0.06 | 12.47 | 217.42 | 2.52 | 1.26 |
| NR-N ³ LO-Idaho | 8.84 | 1.53 | 0.30 | 2.41 | 0.04 | 2.33 | 1.00 | 0.02 | 0.57 | 0.42 | 0.17 | 0.03 | 0.02 |
| NR-N ³ LO-EKM | 16.08 | 13.45 | 0.29 | 0.34 | 0.06 | 0.01 | 0.13 | 0.01 | 0.02 | 0.43 | 0.12 | 1.22 | 0.00 |

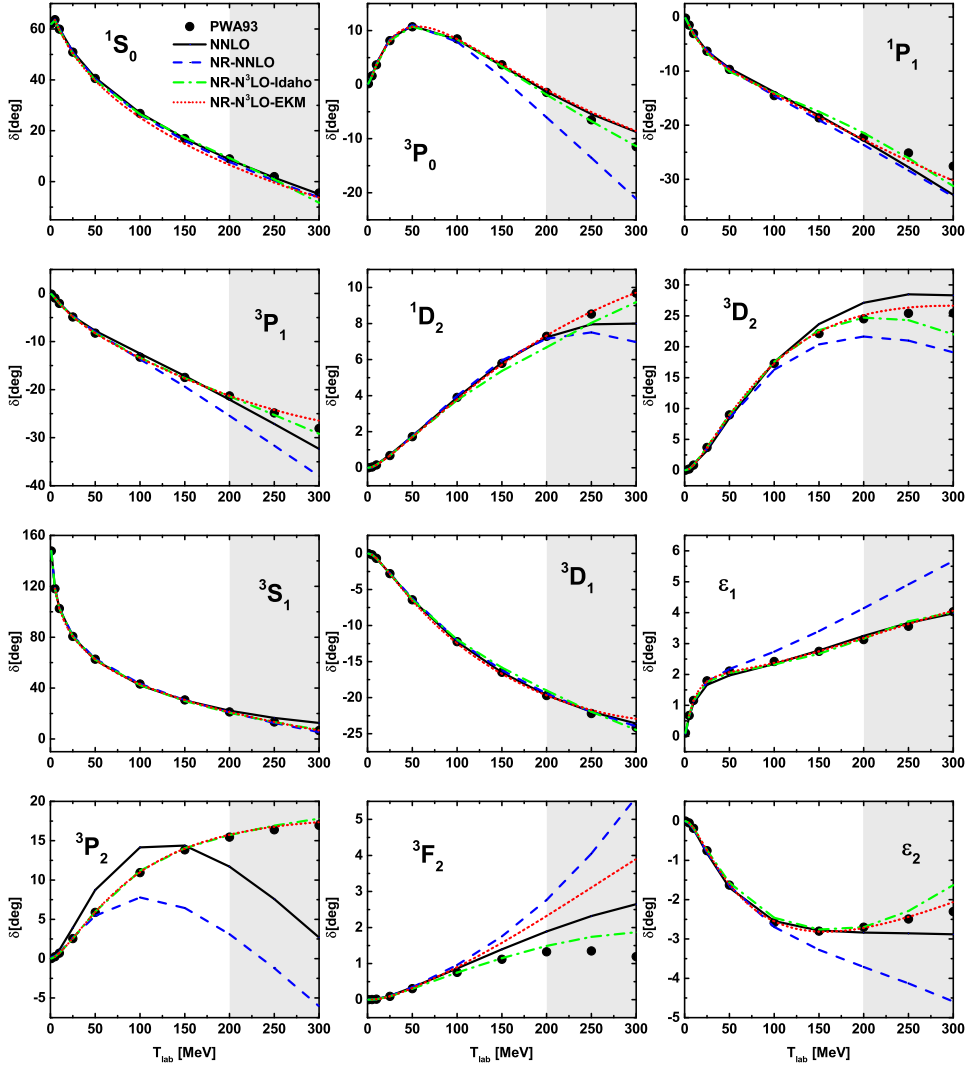


FIG. 1. NN phase shifts for the partial waves with total angular momentum $J \leq 2$. The black solid lines denote the relativistic NNLO results obtained with a cutoff $\Lambda = 0.9$ GeV. For comparison, we also show the non-relativistic results up to NNLO (NR-NNLO, $\Lambda = 0.875$ GeV, blue dashed lines [2]) and N³LO (NR-N³LO-Idaho, $\Lambda = 0.5$ GeV, green dash-dotted lines [3, 4], and NR-N³LO-EKM, $\Lambda = 0.9$ fm, red dotted lines [5, 6]). The black dots denote the empirical PWA93 phase shifts [12]. The shadows represent the energy regions not taken into account in the fitting.

combinations of LECs for the $J = 2$ partial waves instead of three. We have checked that the two combinations D_1 and D_2 only contribute to the 3P_2 and 3P_2 - 3F_2 partial waves, which leads to a much better description of the 3P_2 partial wave. Therefore, in total, we have 19 LECs for the NNLO potential presented in the main text.

INFLUENCE OF CUTOFF VARIATIONS FROM 0.8 GEV TO 0.9 GEV

In Fig. 2, we compare the relativistic NNLO fits obtained with a cutoff of 0.9 GeV and 19 LECs and those obtained with a smaller cutoff of 0.8 GeV. With the cutoff switched to 0.8 GeV, we obtain a relatively better description of 3P_0 , 3D_2 , and 3F_2 for $T_{\text{lab}} \leq 200$ MeV and thus a much smaller $\tilde{\chi}^2 \sim 5.3$. Clearly, the cutoff dependence is visible only for the 3F_2 , 3D_2 phase shifts and the mixing angle ϵ_2 at higher kinetic energies. This indicates that for these partial waves, inclusion of higher chiral order contributions is necessary.

For the 3D_3 partial wave to which no contact term contributes, the phase shifts are more sensitive to the choice of the cutoff as is shown in Fig. 6. This is the main reason why we stick to the cutoff of 0.9 GeV. However, we find that once the N³LO contact terms are introduced, the cutoff dependence can be largely suppressed.

COMPARISON WITH THE BONN POTENTIAL

For years, in relativistic studies of nuclear structure and reactions, the Bonn potential developed in the 1980's has been the only choice [14]. In Figs. 3 and 4, we compare the phase shifts for partial wave with $J \leq 7$. It is clear that on average the relativistic chiral nuclear force provides a better description of the PWA93 phase shifts than the Bonn potential, for example, 1S_0 , 3P_0 , 3D_1 , and 3D_3 .

FIT TO THE GRANADA PWA

In the main text, we have fitted our relativistic chiral nuclear force to the Nijmegen 93 partial wave phase shifts [12], which have been used as benchmark purposes for most previous studies. Starting from 2013 [15], the Granada group has started a new partial wave analysis of the nucleon-nucleon scattering data, employing chiral TPE potentials, providing uncertainties, as well as taking into account correlations [16–18]. As a result, it is interesting to fit our relativistic chiral nuclear force to the Granada phaseshifts [17]. As uncertainties are provided in Ref. [17], we perform a standard χ^2 fit. The results are shown in Fig. 5 labeled as “NNLO-G”, in comparison with the results obtained by fitting to the Nijmegen phase shifts and the N³LO results of Refs. [3–6]. Clearly, we can also obtain satisfactory fits. Comparing the Nijmegen and Granada phaseshifts, one can see some visable differences in

certain channels, such as 3P_2 , 3F_2 , and ϵ_2 , which is mainly due to the fact that charge symmetry breaking is considered for certain P -waves in Ref. [17]. One can see that the two N³LO non-relativistic chiral nuclear forces yield results in better agreement with the Nijmegen PWA results. On the other hand, in the covariant framework, taking into account theoretical uncertainties, the two fits (to either the Nijmegen or the Granada phase shifts) are consistent with each other.

COMPARISON WITH THE NONRELATIVISTIC N³LO RESULTS FOR HIGHER PARTIAL WAVES

In Fig. 6, we compare the NR-N³LO-Idaho [3, 4] and the NR-N³LO-EKM [5, 6] chiral force with the relativistic NNLO chiral force for peripheral partial waves with $J \leq 4$ and $L \leq 4$. Higher partial waves are not explicitly shown since for them the OPE plays the dominant role.

The $\tilde{\chi}^2$ for each partial wave are collected in Table II. Clearly for these partial waves, the relativistic NNLO results are as good as or even slightly better than the nonrelativistic N³LO results for $T_{\text{lab}} \leq 200$ MeV except for 3F_4 . For 3D_3 and 1F_3 , our relativistic NNLO results and NR-N³LO-EKM are not able to describe well the high-momentum data, while the NR-N³LO-Idaho results miss the data for $T_{\text{lab}} \in [100,200]$ MeV. For 3F_3 , no results can reproduce the behavior above $T_{\text{lab}} = 200$ MeV but the NR-N³LO-Idaho results are slightly better. The large part of the $\tilde{\chi}^2$ for our relativistic NNLO results comes from 3F_4 , in which the subleading TPE is strong such that it shifts the results well above the PWA93 phase shifts, while the NR-N³LO-Idaho results behave much better. For the G -waves and the mixing angle ϵ_3 , all three results are in pretty good agreement with the empirical data below $T_{\text{lab}} = 200$ MeV, while the NR-N³LO-Idaho results tend to yield smaller values at higher energies.

Note for the peripheral partial waves shown in Fig. 6, visable differences between the Nijmegen results and the Granada results are found in the 3D_3 , 1F_3 , 3F_3 , and 3G_4 channels. For these partial waves, the chiral phase shifts are predictions. Although the central values of the chiral nuclear forces agree better with the Nijmegen results, considering theoretical uncertainties, they should be viewed more or less equivalent, particularly for laboratory energies smaller than 200 MeV.

THE BAYESIAN MODEL FOR UNCERTAINTY QUANTIFICATION

In this section, we briefly introduce the Bayesian model proposed first in Refs. [19–21] and further improved in Refs. [22–24].

In this approach, one first rewrites an observable X in terms of dimensionless expansion coefficients c_i as

$$X = X_{\text{ref}}(c_0 + c_2 Q^2 + c_3 Q^3 + \dots). \quad (4)$$

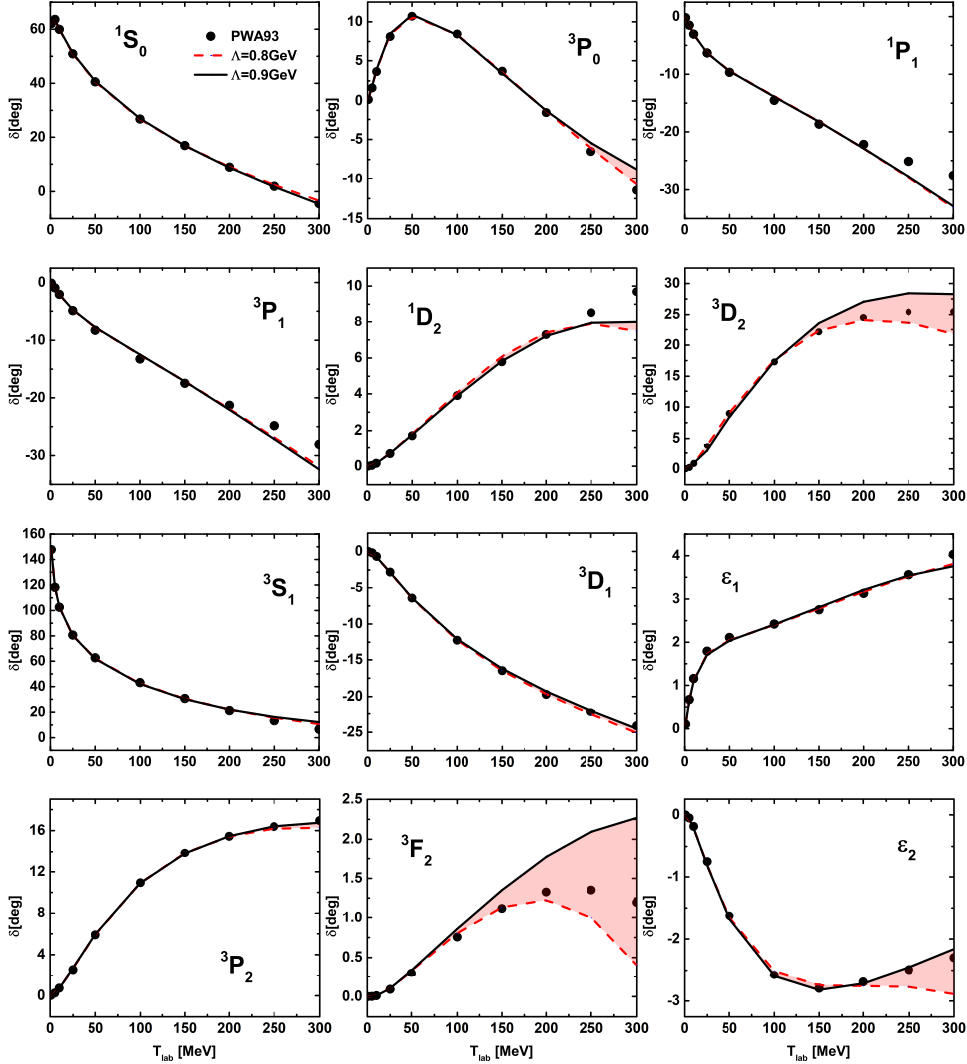


FIG. 2. NN phase shifts for all the partial waves with $J \leq 2$ obtained with a variation of the cutoff from 0.8 GeV to 0.9 GeV. The relativistic NNLO results obtained with a cutoff of $\Lambda = 0.8$ GeV and $\Lambda = 0.9$ GeV are represented with red dashed lines and solid black lines, respectively. The uncertainties due to the cutoff variation are denoted by red shadows.

TABLE II. $\tilde{\chi}^2 = \sum_i (\delta^i - \delta_{\text{PWA93}}^i)^2$ of different chiral forces for partial waves shown in Fig. 6.

| | Total | 3D_3 | 1F_3 | 3F_3 | 3F_4 | 3G_3 | ϵ_3 | 1G_4 | 3G_4 |
|----------------------------|-------|-----------|-----------|-----------|-----------|-----------|--------------|-----------|-----------|
| NNLO | 0.98 | 0.03 | 0.03 | 0.21 | 0.70 | 0.00 | 0.01 | 0.00 | 0.00 |
| NR-N ³ LO-Idaho | 1.73 | 0.58 | 0.73 | 0.13 | 0.12 | 0.00 | 0.01 | 0.01 | 0.15 |
| NR-N ³ LO-EKM | 3.00 | 0.56 | 1.44 | 0.28 | 0.54 | 0.01 | 0.01 | 0.03 | 0.13 |

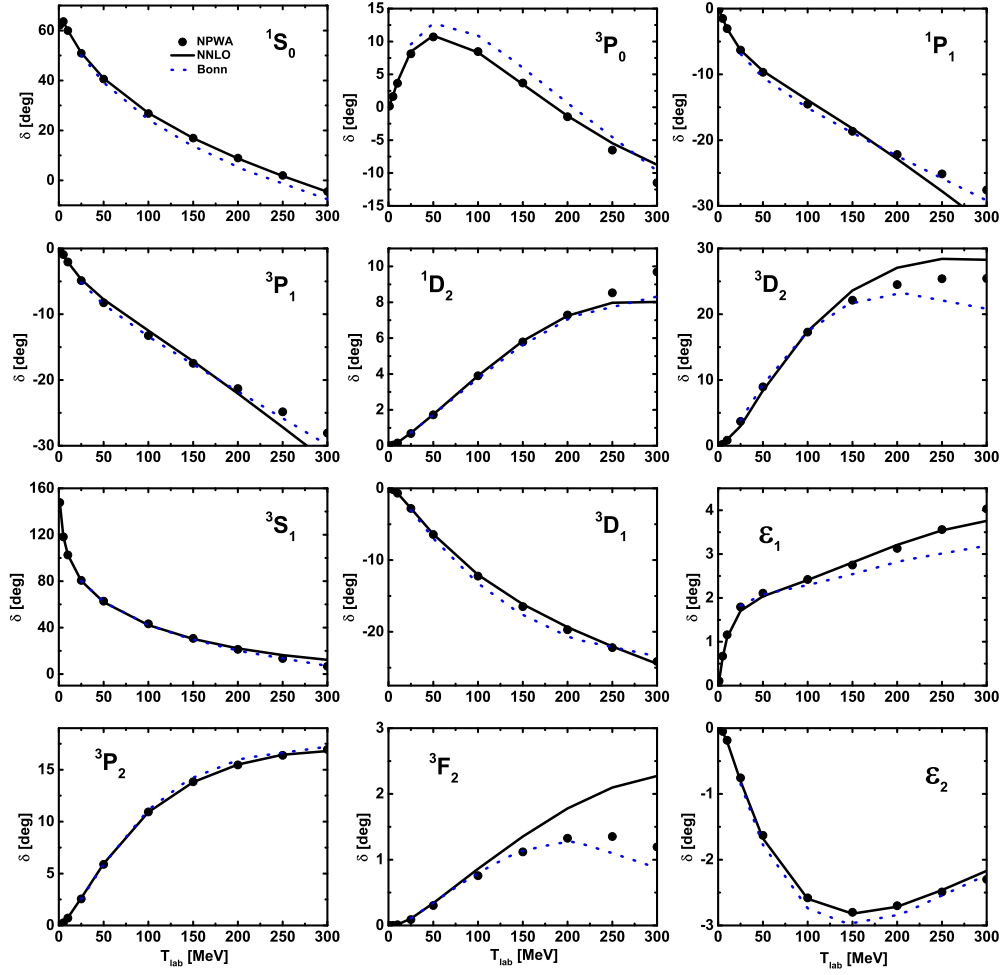


FIG. 3. NN phase shifts for all the partial waves with $J \leq 2$ given by the relativistic NNLO chiral potential and the Bonn potential [13].

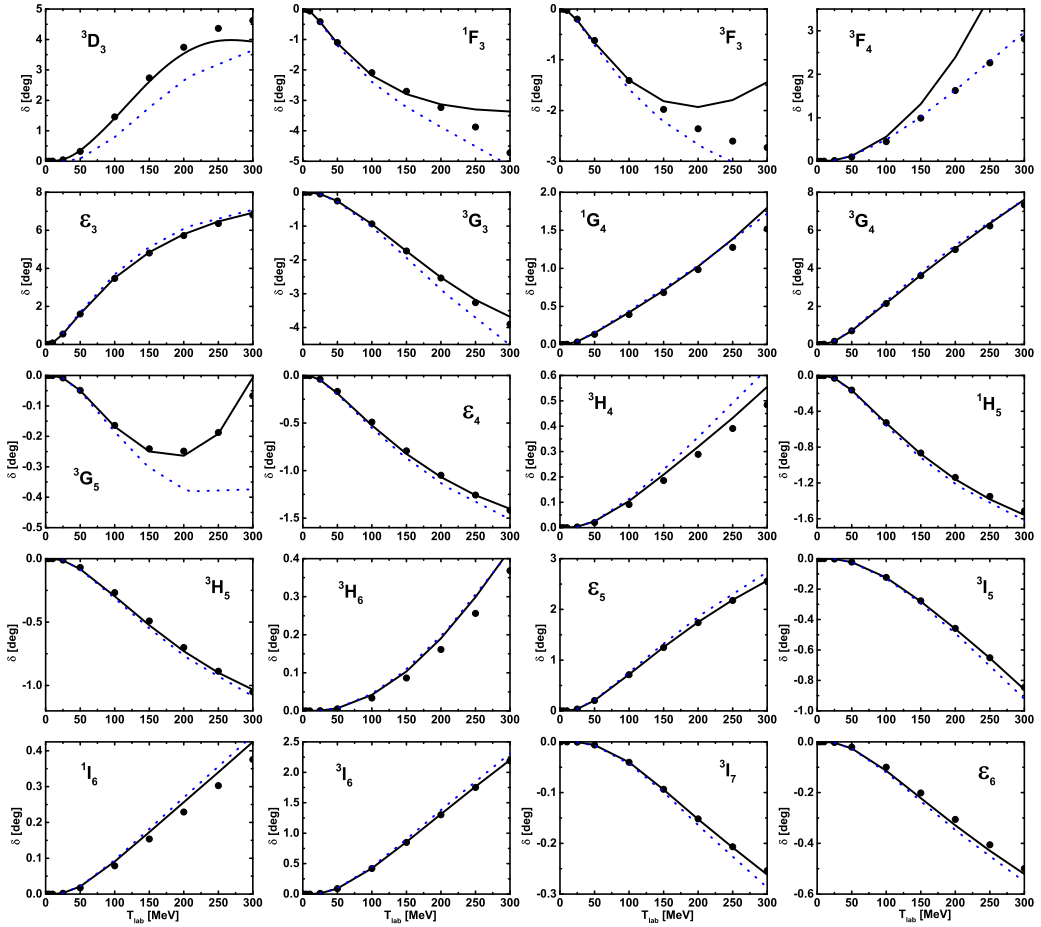


FIG. 4. NN phase shifts for all the partial waves with $3 \leq J \leq 7$ given by the relativistic NNLO chiral potential and the Bonn potential [13].

The chiral expansion parameter Q reads

$$Q = \text{Max}\left\{\frac{p}{\Lambda_b}, \frac{m_\pi}{\Lambda_b}\right\}, \quad (5)$$

where p is the nucleon momentum in the c.m. frame and Λ_b is the cutoff. As is shown in the main text, since the optimum cutoff is determined to be 0.6 GeV at NLO but 0.9 GeV at NNLO, we adopt $\Lambda_b = 0.6$ GeV, which results in more conservative estimates of truncation uncertainties.

More specifically, at NNLO, it is suggested [22] that X_{ref} can be defined as

$$X_{\text{ref}} = \text{Max}\{|X^{\text{LO}}|, \frac{|X^{\text{LO}} - X^{\text{NLO}}|}{Q^2}, \frac{|X^{\text{NLO}} - X^{\text{NNLO}}|}{Q^3}\}, \quad (6)$$

where $c_m = 1, m \in \{0, 2, 3\}$ instead of $X_{\text{ref}} = |X^{\text{LO}}|$ in order to avoid possible underestimation of X_{ref} .

With the assumption that the next h chiral orders dominate the truncation errors and given the knowledge of $\{c_{i \leq k}\}$, the dimensionless residue $\Delta_k \equiv \sum_{n=k+1}^{\infty} c_n Q^n \simeq \sum_{n=k+1}^{k+h} c_n Q^n$ obeys the following probability distribution

$$\text{pr}_h(\Delta | c_{i \leq k}) = \frac{\int_0^\infty d\bar{c} \text{pr}_h(\Delta | \bar{c}) \text{pr}(\bar{c}) \prod_{i \in A} \text{pr}(c_i | \bar{c})}{\int_0^\infty d\bar{c} \text{pr}(\bar{c}) \prod_{i \in A} \text{pr}(c_i | \bar{c})}, \quad (7)$$

with $A = \{n \in \mathbb{N}_0 | n \leq k \wedge n \neq 1 \wedge n \neq m\}$ and

$$\text{pr}_h(\Delta | \bar{c}) = \left[\prod_{i=k+1}^{k+h} \int_{-\infty}^\infty dc_i \text{pr}(c_i | \bar{c}) \right] \delta(\Delta - \sum_{j=k+1}^{k+h} c_j Q^j), \quad (8)$$

where \bar{c} is the hyperparameter for the probability distribution function $\text{pr}(c_i | \bar{c})$, which itself follows the log-uniform proba-

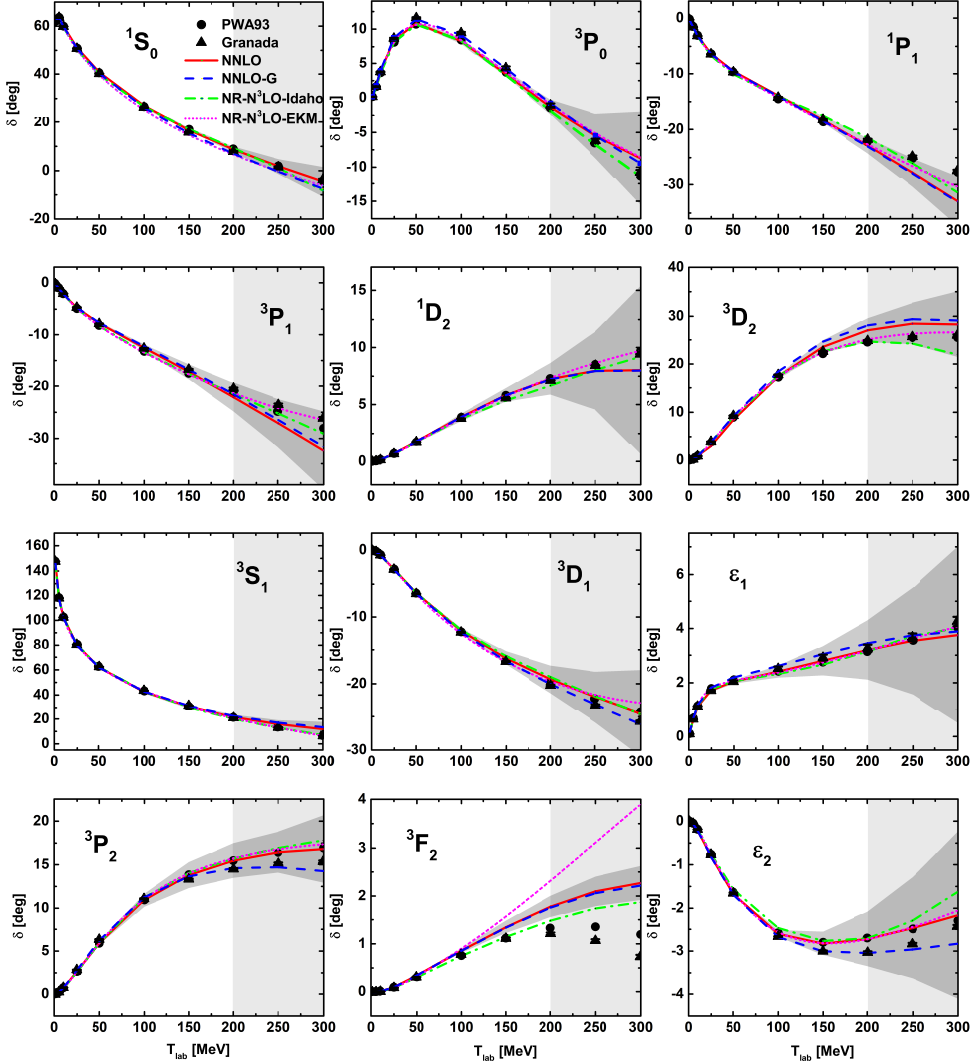


FIG. 5. NN phase shifts for the partial waves with total angular momentum $J \leq 2$. The red solid lines and the gray bands denote the relativistic NNLO results fitting to the empirical PWA93 phase shifts [12] obtained with a cutoff $\Lambda = 0.9$ GeV and 68% DoB truncation errors. The results fitting to the Granada data [17] are depicted with blue dashed lines labeled as “NNLO-G”. For comparison, we also show the non-relativistic results up to $N^3\text{LO}$ (NR-N ^3LO -Idaho, $\Lambda = 0.5$ GeV, green dash-dotted lines [3, 4], and NR-N ^3LO -EKM, $\Lambda = 0.9$ fm, magenta dotted lines [5, 6]). The black solid circles and triangles denote the empirical PWA93 phase shifts [12] and those of the Granada Group [17]. The shadows represent the energy regions not taken into account in the fitting.

bility distribution as

$$\text{pr}(\bar{c}) = \frac{1}{\ln(\bar{c}_>/\bar{c}_<)} \frac{1}{\bar{c}} \theta(\bar{c} - \bar{c}_<) \theta(\bar{c}_> - \bar{c}). \quad (9)$$

Following Refs. [20, 22], we utilize the Gaussian prior for

$\text{pr}(c_i|\bar{c})$ as

$$\text{pr}(c_i|\bar{c}) = \frac{1}{\sqrt{2\pi\bar{c}}} e^{-\frac{c_i^2}{2\bar{c}^2}}. \quad (10)$$

In the practical application, as is suggested in Ref. [20], it is efficient to take $h = 10$, $\bar{c}_< = 0.5$ and $\bar{c}_> = 10.0$. For

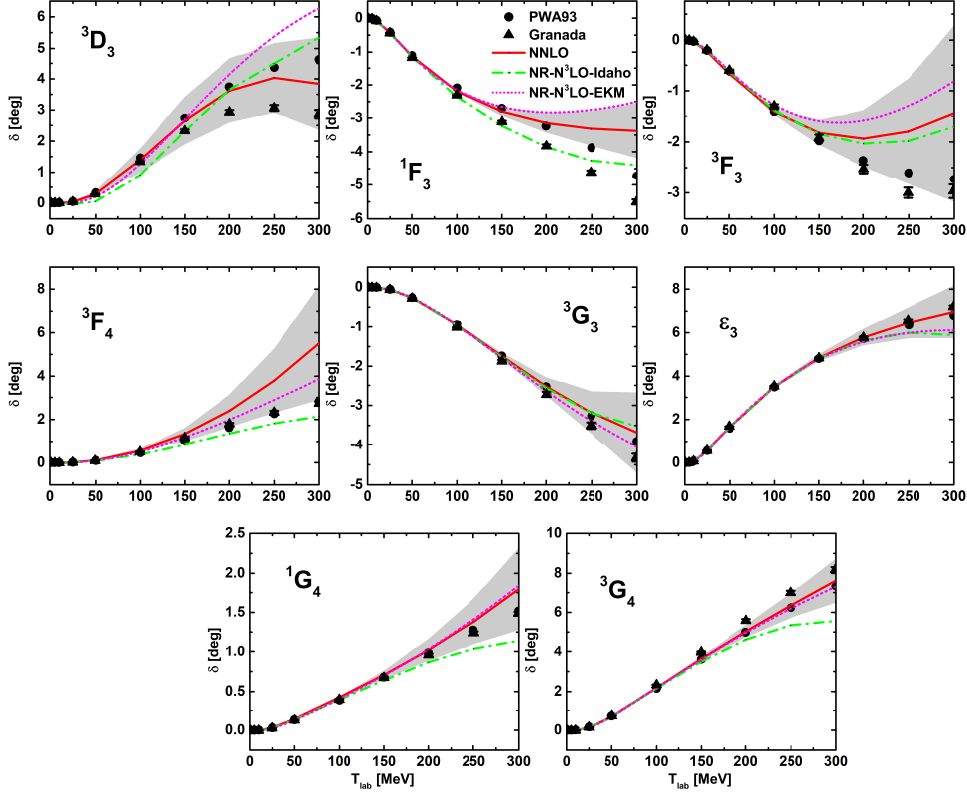


FIG. 6. Same as Fig. 5 but for peripheral partial waves with $J \leq 4$ and $L \leq 4$. Note that for these partial waves, the chiral results are predictions and independent from the partial wave analyses.

any given degree-of-belief (DoB) interval, the truncation uncertainties $\Delta X = X_{\text{ref}}\Delta_k$ can be numerically obtained by integrating over Δ .

CONTACT TERMS

In this section, we explicitly present the partial wave contributions of the LO and NLO contact terms of our relativistic chiral nuclear force. For simplification, we define

$$\Delta_p = E_p - m, \quad \Delta_{p'} = E_{p'} - m, \quad (11)$$

$$N_p = E_p + m, \quad N_{p'} = E_{p'} + m, \quad (12)$$

$$\Sigma = E_p E_{p'} + m^2, \quad \Gamma = E_p E_{p'} - m^2. \quad (13)$$

The contributions of contact terms to each partial wave then read

$$\begin{aligned}
 V_{1S0}^{LO} &= 2\pi \left(2C_1^{1S0} + C_2^{1S0} \frac{\Gamma}{m^2} \right) \\
 V_{3P0}^{LO} &= -\frac{2\pi C^{3P0} pp'}{m^2} \\
 V_{1P1}^{LO} &= -\frac{2\pi C^{1P1} pp'}{3m^2} \\
 V_{3P1}^{LO} &= -\frac{4\pi C^{3P1} pp'}{3m^2} \\
 V_{3S1}^{LO} &= C_1^{3S1} \frac{4\pi (7m^2 + 2m(E_p + E_{p'}) - 2E_p E_{p'})}{9m^2} \\
 &\quad + C_2^{3S1} \frac{2}{3}\pi \frac{\Gamma}{m^2} \\
 V_{3D1}^{LO} &= C^{3D1} \frac{8\pi \Delta_p \Delta_{p'}}{9m^2} \\
 V_{3SD1}^{LO} &= \frac{2\sqrt{2}\pi \Delta_{p'} (6mC_1^{3SD1} + C_2^{3SD1} \Delta_p)}{9m^2}
 \end{aligned} \tag{14}$$

$$\begin{aligned}
V_{1S0}^{NLO} = & C_1^{1S0} + C_2^{1S0} \frac{(\Delta_p + \Delta_{p'})}{m} \\
& + C_3^{1S0} \frac{(p^2 \Delta_p E_{p'} + p'^2 \Delta_{p'} E_p)}{m^4} \\
& + C_4^{1S0} \frac{p^2 p'^2}{m^2 N_p N_{p'}} + C_5^{1S0} \frac{\Sigma \sqrt{s} (\Delta_p + \Delta_{p'})}{m^4} \\
& + C_6^{1S0} \frac{\sqrt{s} \Delta_p \Delta_{p'}}{m^3} + C_7^{1S0} \frac{(s + \Delta_p E_p + \Delta_{p'} E_{p'})}{m^2} \\
& + C_8^{1S0} \frac{\Gamma s}{m^4} + C_9^{1S0} \frac{(\Delta_p E_p + \Delta_{p'} E_{p'})}{m^2} \\
& + C_{10}^{1S0} \frac{\Delta_p \Delta_{p'} (E_p + E_{p'})}{m^3} + C_{11}^{1S0} \frac{\Delta_p \Delta_{p'} E_p E_{p'}}{m^4}
\end{aligned} \tag{15}$$

$$\begin{aligned}
V_{3P0}^{NLO} = & C_1^{3P0} \frac{pp'}{m^2} + C_2^{3P0} \frac{pp'(\Delta_p + \Delta_{p'})}{m^3} \\
& + C_3^{3P0} \frac{p^3 p'^3}{m^4 N_p N_{p'}} + C_4^{3P0} \frac{pp' \sqrt{s}}{m^3} \\
& + C_5^{3P0} \frac{pp' \sqrt{s} (\Delta_p + \Delta_{p'})}{m^4} + C_6^{3P0} \frac{pp' s}{m^4} \\
& + C_7^{3P0} \frac{pp' (\Delta_p E_p + \Delta_{p'} E_{p'})}{m^4}
\end{aligned} \tag{16}$$

$$\begin{aligned}
V_{1P1}^{NLO} = & C_1^{1P1} \frac{pp'}{m^2} + C_2^{1P1} \frac{pp'(\Delta_p + \Delta_{p'})}{m^3} \\
& + C_3^{1P1} \frac{p^3 p'^3}{m^4 N_p N_{p'}} + C_4^{1P1} \frac{pp' \sqrt{s} (E_p + E_{p'})}{m^4} \\
& + C_5^{1P1} \frac{pp' s}{m^4} + C_6^{1P1} \frac{pp' (\Delta_p E_p + \Delta_{p'} E_{p'})}{m^4}
\end{aligned} \tag{17}$$

$$\begin{aligned}
V_{3P1}^{NLO} = & C_1^{3P1} \frac{pp'}{m^2} + C_2^{3P1} \frac{pp'(\Delta_p + \Delta_{p'})}{m^3} \\
& + C_3^{3P1} \frac{p^3 p'^3}{m^4 N_p N_{p'}} + C_4^{3P1} \frac{pp' \sqrt{s} (E_p + E_{p'})}{m^4} \\
& + C_5^{3P1} \frac{pp' s}{m^4} + C_6^{3P1} \frac{pp' (\Delta_p E_p + \Delta_{p'} E_{p'})}{m^4}
\end{aligned} \tag{18}$$

$$\begin{aligned}
V_{3S1}^{NLO} = & C_1^{3S1} \frac{\Delta_p + \Delta_{p'}}{m} + C_2^{3S1} \frac{p^2 \Delta_p + p'^2 \Delta_{p'}}{m^3} \\
& + C_3^{3S1} \frac{p^2 p'^2}{m^2 N_p N_{p'}} + C_4^{3S1} \frac{\Delta_p \Delta_{p'} (p^2 + p'^2)}{m^4} \\
& + C_5^{3S1} \frac{\sqrt{s} (p^2 + p'^2)}{m^3} + C_6^{3S1} \frac{\sqrt{s} \Delta_p \Delta_{p'}}{m^3} \\
& + C_7^{3S1} \frac{-4m^2 + s + \Delta_p E_p + \Delta_{p'} E_{p'}}{m^2} \\
& + C_8^{3S1} \frac{s (\Delta_p + \Delta_{p'})}{m^3} + C_9^{3S1} \frac{s \Delta_p \Delta_{p'}}{m^4} \\
& + C_{10}^{3S1} \frac{\Delta_p E_p + \Delta_{p'} E_{p'}}{m^2} + C_{11}^{3S1} \frac{\Delta_p \Delta_{p'} (E_p + E_{p'})}{m^3} \\
& + C_{12}^{3S1} \frac{\sqrt{s} \Delta_p \Delta_{p'} (E_p + E_{p'})}{m^4} + C_{13}^{3S1} \frac{\Delta_p \Delta_{p'} E_p E_{p'}}{m^4}
\end{aligned} \tag{19}$$

$$\begin{aligned}
V_{3D1}^{NLO} = & C_1^{3D1} \frac{\Delta_p \Delta_{p'}}{m^2} + C_2^{3D1} \frac{\Delta_p \Delta_{p'} (p^2 + p'^2)}{m^4} \\
& + C_3^{3D1} \frac{\sqrt{s} (p^2 \Delta_{p'} + p'^2 \Delta_p)}{2m^4} + C_4^{3D1} \frac{p^2 p'^2 s}{m^4 N_p N_{p'}} \\
& + C_5^{3D1} \frac{\Delta_p \Delta_{p'} (E_p + E_{p'})}{m^3} + C_6^{3D1} \frac{\Delta_p \Delta_{p'} E_p E_{p'}}{m^4}
\end{aligned} \tag{20}$$

$$\begin{aligned}
V_{3SD1}^{NLO} = & C_1^{3SD1} \frac{\sqrt{2} \Delta_{p'}}{9m} + C_2^{3SD1} \frac{\sqrt{2} \Delta_{p'}^2 N_{p'}}{9m^3} \\
& + C_3^{3SD1} \frac{\sqrt{2} \Delta_p \Delta_{p'}}{9m^2} + C_4^{3SD1} \frac{\sqrt{2} \Delta_p \Delta_{p'} (p^2 + p'^2)}{9m^4} \\
& + C_5^{3SD1} \frac{\sqrt{2s} \Delta_{p'} (\sqrt{s} + N_{p'})}{9m^3} \\
& + C_6^{3SD1} \frac{\sqrt{2s} \Delta_p \Delta_{p'}}{9m^3} + C_7^{3SD1} \frac{\sqrt{2s} \Delta_{p'}}{9m^3} \\
& + C_8^{3SD1} \frac{\sqrt{2s} \Delta_p \Delta_{p'}}{9m^4} + C_9^{3SD1} \frac{\sqrt{2} \Delta_{p'} E_{p'}}{9m^2} \\
& + C_{10}^{3SD1} \frac{\sqrt{2} \Delta_p \Delta_{p'} E_{p'}}{9m^3} + C_{11}^{3SD1} \frac{\sqrt{2s} \Delta_p \Delta_{p'} (E_p + E_{p'})}{9m^4} \\
& + C_{12}^{3SD1} \frac{\sqrt{2} \Delta_p \Delta_{p'} E_p}{9m^3} \\
& + C_{13}^{3SD1} \frac{\sqrt{2} \Delta_p \Delta_{p'} E_p E_{p'}}{9m^4}
\end{aligned} \tag{21}$$

$$\begin{aligned}
V_{1D2}^{NLO} = & \frac{C^{1D2} p^2 p'^2}{m^4} \\
V_{3D2}^{NLO} = & \frac{C^{3D2} p^2 p^2}{m^4} \\
V_{3P2}^{NLO} = & C_1^{3P2} \frac{pp'}{m^2} + C_2^{3P2} \frac{pp'(\Delta_p + \Delta_{p'})}{m^3} \\
& + C_3^{3P2} \frac{p^3 p'^3}{m^4 N_p N_{p'}}
\end{aligned} \tag{22}$$

$$\begin{aligned}
V_{3P2-3F2}^{NLO} = & C_1^{3PF2} \frac{2 \sqrt{\frac{2}{3}} pp'^3}{25 m^3 N_{p'}} \\
& + C_2^{3PF2} \frac{\sqrt{\frac{2}{3}} p^3 p'^3}{25 m^4 N_p N_{p'}}
\end{aligned}$$

Note that a factor of π is omitted in Eqs. (15-22). The partial wave combinations in terms of the LECs appear in the covariant Lagrangians are given as follows.

$$\begin{aligned}
C_1^{1S0} &= O_1 + O_2 + 3O_3 - 6O_4 \\
C_2^{1S0} &= O_1 + 4(O_2 + O_3 - 3O_4) \\
C_3^{1P0} &= O_1 - 4(O_2 + O_3 + 3O_4) \\
C_4^{1P1} &= O_1 + 4O_4 \\
C_5^{3P1} &= O_1 - 2O_2 + 2O_3 \\
C_6^{3S1} &= O_1 + O_2 - O_3 + 2O_4 \\
C_7^{3S1} &= 3O_1 + 4O_2 - 4O_3 - 4O_4 \\
C_8^{3D1} &= O_1 + O_2 - O_3 + 2O_4 \\
C_9^{3SD1} &= O_1 + O_2 - O_3 + 2O_4 \\
C_{10}^{3SD1} &= O_1 + 4O_2 - 4O_3 - 4O_4
\end{aligned} \tag{23}$$

$$\begin{aligned}
C_1^{3P0} &= \frac{2O_{10}}{3} + \frac{2O_{11}}{3} - \frac{2O_{12}}{3} + \frac{4O_{13}}{3} + \frac{8O_{14}}{3} - \frac{22O_{15}}{3} \\
&\quad - \frac{26O_{16}}{3} - \frac{68O_{17}}{3} - 2O_5 + 2O_6 + \frac{8O_7}{3} - \frac{8O_8}{3} + \frac{8O_9}{3} \\
C_2^{3P0} &= \frac{5O_{10}}{6} - 2O_{11} - 2O_{12} - \frac{14O_{13}}{3} - \frac{O_{14}}{6} + 2O_{15} \\
&\quad + 2O_{16} + \frac{22O_{17}}{3} + \frac{3O_6}{2} + \frac{11O_7}{6} - \frac{4O_8}{3} - \frac{7O_9}{6} \\
C_3^{3P0} &= \frac{O_{10}}{3} + \frac{4O_{13}}{3} + \frac{O_{14}}{3} + \frac{4O_{17}}{3} + O_6 + \frac{O_7}{3} \\
&\quad - \frac{4O_8}{3} + \frac{O_9}{3} \\
C_4^{3P0} &= 4O_6 + 8O_7 - 4O_8 \\
C_5^{3P0} &= 2O_6 + 4O_7 - 2O_8 \\
C_6^{3P0} &= -\frac{O_{14}}{2} + 2O_{15} + 2O_{16} + 6O_{17} + 2O_6 + 6O_7 \\
C_7^{3P0} &= \frac{O_{10}}{2} - 2O_{11} - 2O_{12} - 6O_{13} - \frac{O_{14}}{2} + 2O_{15} \\
&\quad + 2O_{16} + 6O_{17} + \frac{O_6}{2} + \frac{3O_7}{2} - \frac{3O_9}{2}
\end{aligned} \tag{25}$$

$$\begin{aligned}
C_1^{1S0} &= -4O_{14} - 4O_{15} - 12O_{16} + 24O_{17} \\
C_2^{1S0} &= -O_{10} - O_{11} - 3O_{12} + 6O_{13} - O_{14} \\
&\quad - 7O_{15} - 5O_{16} + 18O_{17} + 2O_5 + O_6 - 2O_7 + 2O_9 \\
C_3^{1S0} &= -\frac{O_{10}}{2} - 2O_{11} - 2O_{12} + 6O_{13} + \frac{O_{14}}{2} + 2O_{15} \\
&\quad + 2O_{16} - 6O_{17} + \frac{O_6}{2} - \frac{3O_7}{2} + \frac{3O_9}{2} \\
C_4^{1S0} &= -\frac{4O_{10}}{3} - 4O_{11} - 4O_{12} + \frac{32O_{13}}{3} - \frac{4O_{14}}{3} - 4O_{15} \\
&\quad - 4O_{16} + \frac{32O_{17}}{3} + 2O_5 + 2O_6 - \frac{10O_7}{3} + \frac{4O_8}{3} + \frac{8O_9}{3} \\
C_5^{1S0} &= 2O_6 - 4O_7 + 2O_8 \\
C_6^{1S0} &= 4O_6 - 8O_7 + 4O_8 \\
C_7^{1S0} &= O_{14} + O_{15} + 3O_{16} - 6O_{17} \\
C_8^{1S0} &= \frac{O_{14}}{2} + 2O_{15} + 2O_{16} - 6O_{17} + 2O_6 - 6O_7 \\
C_9^{1S0} &= -O_{10} - O_{11} - 3O_{12} + 6O_{13} + O_6 - 2O_7 + 2O_9 \\
C_{10}^{1S0} &= -\frac{5O_{10}}{6} - 2O_{11} - 2O_{12} + \frac{14O_{13}}{3} + \frac{O_{14}}{6} + 2O_{15} \\
&\quad + 2O_{16} - \frac{22O_{17}}{3} + \frac{3O_6}{2} - \frac{11O_7}{6} + \frac{4O_8}{3} + \frac{7O_9}{6} \\
C_{11}^{1S0} &= -\frac{O_{10}}{3} - \frac{4O_{13}}{3} - \frac{O_{14}}{3} - \frac{4O_{17}}{3} + O_6 - \frac{O_7}{3} \\
&\quad + \frac{4O_8}{3} - \frac{O_9}{3}
\end{aligned} \tag{24}$$

$$\begin{aligned}
C_1^{1P1} &= \frac{2O_{10}}{3} + \frac{2O_{11}}{3} + 2O_{12} - 4O_{13} + \frac{4O_{14}}{3} + \frac{2O_{15}}{3} \\
&\quad + 2O_{16} - \frac{4O_{17}}{3} - \frac{2O_5}{3} + \frac{2O_6}{3} - \frac{4O_7}{3} - \frac{4O_9}{3} \\
C_2^{1P1} &= \frac{O_{10}}{2} + \frac{4O_{11}}{3} + \frac{4O_{12}}{3} - \frac{10O_{13}}{3} + \frac{O_{14}}{6} + \frac{4O_{15}}{3} \\
&\quad + \frac{4O_{16}}{3} - \frac{14O_{17}}{3} + \frac{O_6}{2} - \frac{7O_7}{6} - \frac{5O_9}{6} \\
C_3^{1P1} &= \frac{O_{10}}{3} + \frac{4O_{11}}{3} + \frac{4O_{12}}{3} - 4O_{13} + \frac{O_{14}}{3} + \frac{4O_{15}}{3} \\
&\quad + \frac{4O_{16}}{3} - 4O_{17} + \frac{O_6}{3} - O_7 - O_9 \\
C_4^{1P1} &= \frac{2O_6}{3} - \frac{4O_7}{3} - \frac{2O_8}{3} \\
C_5^{1P1} &= -\frac{O_{14}}{6} - \frac{2O_{17}}{3} + \frac{2O_6}{3} - \frac{2O_7}{3} \\
C_6^{1P1} &= \frac{O_{10}}{6} + \frac{2O_{13}}{3} - \frac{O_{14}}{6} - \frac{2O_{17}}{3} + \frac{O_6}{6} - \frac{O_7}{6} + \frac{O_9}{6}
\end{aligned} \tag{26}$$

$$\begin{aligned}
C_1^{3P1} &= \frac{2O_{10}}{3} + \frac{2O_{11}}{3} - \frac{2O_{12}}{3} + \frac{4O_{13}}{3} + 2O_{14} - 2O_{15} \\
&\quad + 2O_{16} + \frac{4O_{17}}{3} + \frac{4O_5}{3} - \frac{4O_6}{3} - \frac{2O_7}{3} - \frac{4O_8}{3} - \frac{2O_9}{3} \\
C_2^{3P1} &= \frac{2O_{10}}{3} + \frac{4O_{15}}{3} - \frac{4O_{16}}{3} - O_6 - \frac{2O_7}{3} \\
&\quad - \frac{2O_8}{3} - \frac{4O_9}{3} \\
C_3^{3P1} &= \frac{O_{10}}{3} + \frac{2O_{11}}{3} - \frac{2O_{12}}{3} + \frac{O_{14}}{3} + \frac{2O_{15}}{3} - \frac{2O_{16}}{3} \\
&\quad - \frac{2O_6}{3} - O_7 - \frac{2O_8}{3} - O_9 \\
C_4^{3P1} &= -\frac{4O_6}{3} - \frac{4O_8}{3} \\
C_5^{3P1} &= -\frac{O_{14}}{3} + \frac{2O_{15}}{3} - \frac{2O_{16}}{3} - \frac{4O_6}{3} + \frac{4O_7}{3} \\
C_6^{3P1} &= \frac{O_{10}}{3} - \frac{2O_{11}}{3} + \frac{2O_{12}}{3} - \frac{O_{14}}{3} + \frac{2O_{15}}{3} - \frac{2O_{16}}{3} \\
&\quad - \frac{O_6}{3} + \frac{O_7}{3} - \frac{O_9}{3}
\end{aligned} \tag{27}$$

$$\begin{aligned}
C_1^{3S1} &= -O_{10} - O_{11} + O_{12} - 2O_{13} - O_{14} - \frac{5O_{15}}{3} \\
&\quad + \frac{5O_{16}}{3} - \frac{2O_{17}}{3} - \frac{2O_5}{3} - \frac{O_6}{3} + \frac{2O_7}{3} - \frac{2O_9}{3} \\
C_2^{3S1} &= -\frac{O_{10}}{2} - \frac{2O_{11}}{3} + \frac{2O_{12}}{3} - \frac{2O_{13}}{3} + \frac{O_{14}}{2} + \frac{2O_{15}}{3} \\
&\quad - \frac{2O_{16}}{3} + \frac{2O_{17}}{3} - \frac{O_6}{6} - \frac{O_7}{6} + \frac{O_9}{6} \\
C_3^{3S1} &= -\frac{4O_{10}}{3} - \frac{4O_{11}}{9} + \frac{4O_{12}}{3} - \frac{4O_{14}}{9} + \frac{4O_{15}}{9} + \frac{4O_{16}}{9} \\
&\quad + \frac{16O_{17}}{9} - \frac{2O_5}{3} - \frac{2O_6}{3} + \frac{14O_7}{9} + \frac{4O_8}{9} + \frac{4O_9}{9} \\
C_4^{3S1} &= -\frac{5O_{10}}{18} - \frac{4O_{11}}{9} + \frac{4O_{12}}{9} - \frac{2O_{13}}{9} + \frac{5O_{14}}{18} + \frac{4O_{15}}{9} \\
&\quad - \frac{4O_{16}}{9} + \frac{2O_{17}}{9} - \frac{O_6}{6} - \frac{O_7}{6} + \frac{O_9}{6} \\
C_5^{3S1} &= -\frac{2O_6}{3} + \frac{4O_7}{3} + 2O_8 \\
C_6^{3S1} &= -\frac{4O_6}{3} + \frac{8O_7}{9} + \frac{20O_8}{9} \\
C_7^{3S1} &= O_{14} + O_{15} - O_{16} + 2O_{17} \\
C_8^{3S1} &= \frac{O_{14}}{2} + \frac{2O_{15}}{3} - \frac{2O_{16}}{3} + \frac{2O_{17}}{3} - \frac{2O_6}{3} - \frac{2O_7}{3} \\
C_9^{3S1} &= \frac{5O_{14}}{18} + \frac{4O_{15}}{9} - \frac{4O_{16}}{9} + \frac{2O_{17}}{9} - \frac{2O_6}{3} - \frac{2O_7}{3} \\
C_{10}^{3S1} &= -O_{10} - O_{11} + O_{12} - 2O_{13} - \frac{O_6}{3} + \frac{2O_7}{3} - \frac{2O_9}{3} \\
C_{11}^{3S1} &= -\frac{5O_{10}}{6} + \frac{2O_{11}}{9} + \frac{2O_{12}}{3} + \frac{2O_{13}}{3} + \frac{O_{14}}{6} + \frac{14O_{15}}{9} \\
&\quad - \frac{2O_{16}}{3} + 2O_{17} - \frac{O_6}{2} + \frac{23O_7}{18} + \frac{4O_8}{9} + \frac{13O_9}{18} \\
C_{12}^{3S1} &= -\frac{2O_6}{3} + \frac{4O_7}{9} + \frac{10O_8}{9} \\
C_{13}^{3S1} &= -\frac{O_{10}}{3} + \frac{8O_{11}}{9} + \frac{4O_{13}}{3} - \frac{O_{14}}{3} + \frac{8O_{15}}{9} + \frac{4O_{17}}{3} \\
&\quad - \frac{O_6}{3} + O_7 + \frac{4O_8}{9} + O_9
\end{aligned} \tag{28}$$

$$\begin{aligned}
C_1^{3D1} &= -\frac{O_{10}}{3} + \frac{10O_{11}}{9} + \frac{2O_{12}}{3} + \frac{8O_{13}}{3} - \frac{11O_{14}}{9} \\
&\quad + \frac{2O_{15}}{9} + \frac{14O_{16}}{9} + \frac{8O_{17}}{9} + \frac{O_7}{9} + \frac{2O_8}{9} + \frac{17O_9}{9} \\
C_2^{3D1} &= -\frac{2O_{10}}{9} - \frac{2O_{11}}{9} + \frac{2O_{12}}{9} - \frac{4O_{13}}{9} + \frac{2O_{14}}{9} + \frac{2O_{15}}{9} \\
&\quad - \frac{2O_{16}}{9} + \frac{4O_{17}}{9} \\
C_3^{3D1} &= \frac{16O_7}{9} + \frac{16O_8}{9} \\
C_4^{3D1} &= \frac{2O_{14}}{9} + \frac{2O_{15}}{9} - \frac{2O_{16}}{9} + \frac{4O_{17}}{9} \\
C_5^{3D1} &= -\frac{O_{10}}{3} + \frac{10O_{11}}{9} + \frac{2O_{12}}{3} + \frac{8O_{13}}{3} - \frac{O_{14}}{3} + \frac{10O_{15}}{9} \\
&\quad + \frac{2O_{16}}{3} + \frac{8O_{17}}{3} + \frac{5O_7}{9} + \frac{2O_8}{9} + \frac{13O_9}{9} \\
C_6^{3D1} &= -\frac{O_{10}}{3} + \frac{10O_{11}}{9} + \frac{2O_{12}}{3} + \frac{8O_{13}}{3} - \frac{O_{14}}{3} + \frac{10O_{15}}{9} \\
&\quad + \frac{2O_{16}}{3} + \frac{8O_{17}}{3} + O_7 + \frac{2O_8}{9} + O_9
\end{aligned} \tag{29}$$

$$\begin{aligned}
C_1^{3SD1} &= -12O_{15} + 12O_{16} + 24O_{17} - 12O_5 \\
&\quad - 6O_6 - 6O_7 + 6O_9 \\
C_2^{3SD1} &= -3O_{11} + 3O_{12} + 6O_{13} + 3O_{15} - 3O_{16} \\
&\quad - 6O_{17} - 3O_6 - 3O_7 + 3O_9 \\
C_3^{3SD1} &= -5O_{11} - 3O_{12} - 6O_{13} - 2O_{14} - 7O_{15} \\
&\quad - O_{16} - 10O_{17} - 6O_5 - 6O_6 - 5O_7 + 2O_8 + 5O_9 \\
C_4^{3SD1} &= -\frac{O_{10}}{2} - 2O_{11} + 2O_{12} + 2O_{13} + \frac{O_{14}}{2} + 2O_{15} \\
&\quad - 2O_{16} - 2O_{17} - \frac{3O_6}{2} - \frac{3O_7}{2} + \frac{3O_9}{2} \\
C_5^{3SD1} &= -12O_6 - 12O_7 \\
C_6^{3SD1} &= -12O_6 - 8O_7 + 4O_8 \\
C_7^{3SD1} &= 3O_{15} - 3O_{16} - 6O_{17} \\
C_8^{3SD1} &= \frac{O_{14}}{2} + 2O_{15} - 2O_{16} - 2O_{17} - 6O_6 - 6O_7 \\
C_9^{3SD1} &= -6O_6 - 6O_7 + 6O_9 \\
C_{10}^{3SD1} &= -2O_{11} - 6O_{12} - 12O_{13} - 2O_{15} - 6O_{16} \\
&\quad - 12O_{17} - 6O_6 - 4O_7 + 2O_8 + 4O_9 \\
C_{11}^{3SD1} &= -6O_6 - 4O_7 + 2O_8 \\
C_{12}^{3SD1} &= -5O_{11} - 3O_{12} - 6O_{13} + O_{15} - 9O_{16} \\
&\quad - 18O_{17} - 3O_6 - O_7 + 2O_8 + O_9 \\
C_{13}^{3SD1} &= -2O_{11} - 6O_{12} - 12O_{13} - 2O_{15} - 6O_{16} \\
&\quad - 12O_{17} - 3O_6 + 2O_8
\end{aligned} \tag{30}$$

$$\begin{aligned}
C^{1D2} &= -\frac{2O_{10}}{15} - \frac{8O_{13}}{15} - \frac{2O_{14}}{15} - \frac{8O_{17}}{15} - \frac{2O_7}{15} \\
&\quad - \frac{4O_8}{15} - \frac{2O_9}{15} \\
C^{3D2} &= -\frac{O_{10}}{5} + \frac{2O_{11}}{5} - \frac{2O_{12}}{5} - \frac{O_{14}}{5} + \frac{2O_{15}}{5} - \frac{2O_{16}}{5} \\
&\quad - \frac{O_7}{5} - \frac{2O_8}{5} - \frac{O_9}{5} \\
C_1^{3P2} &= \frac{2O_{10}}{75} + \frac{2O_{11}}{75} - \frac{2O_{12}}{75} + \frac{4O_{13}}{75} + \frac{2O_{14}}{75} + \frac{2O_{15}}{75} \\
&\quad - \frac{2O_{16}}{75} + \frac{4O_{17}}{75} + \frac{2O_7}{75} + \frac{4O_8}{75} + \frac{2O_9}{75} \\
C_2^{3P2} &= \frac{O_{10}}{75} + \frac{2O_{11}}{25} - \frac{2O_{12}}{25} - \frac{8O_{13}}{75} + \frac{O_{14}}{75} + \frac{2O_{15}}{25} \\
&\quad - \frac{2O_{16}}{25} - \frac{8O_{17}}{75} + \frac{O_7}{75} + \frac{2O_8}{75} + \frac{O_9}{75} \\
C_3^{3P2} &= \frac{13O_{10}}{75} + \frac{6O_{11}}{25} - \frac{6O_{12}}{25} + \frac{16O_{13}}{75} + \frac{13O_{14}}{75} \\
&\quad + \frac{6O_{15}}{25} - \frac{6O_{16}}{25} + \frac{16O_{17}}{75} + \frac{13O_7}{75} + \frac{26O_8}{75} + \frac{13O_9}{75} \\
C^{3F2} &= \frac{4O_{10}}{25} + \frac{4O_{11}}{25} - \frac{4O_{12}}{25} + \frac{8O_{13}}{25} + \frac{4O_{14}}{25} + \frac{4O_{15}}{25} \\
&\quad - \frac{4O_{16}}{25} + \frac{8O_{17}}{25} + \frac{4O_7}{25} + \frac{8O_8}{25} + \frac{4O_9}{25} \\
C_1^{3PF2} &= 5O_{11} - 5O_{12} - 10O_{13} + 5O_{15} - 5O_{16} - 10O_{17} \\
C_2^{3PF2} &= O_{10} + 6O_{11} - 6O_{12} - 8O_{13} + O_{14} + 6O_{15} \\
&\quad - 6O_{16} - 8O_{17} + O_7 + 2O_8 + O_9
\end{aligned} \tag{31}$$

-
- [1] Y. Xiao, L.-S. Geng, and X.-L. Ren, Phys. Rev. C **99**, 024004 (2019), arXiv:1812.03005 [nucl-th].
- [2] E. Epelbaum, W. Gloeckle, and U.-G. Meißner, Nucl. Phys. A **671**, 295 (2000).
- [3] D. R. Entem and R. Machleidt, Phys. Rev. C **68**, 041001 (2003).
- [4] R. Machleidt and D. R. Entem, Phys. Rept. **503**, 1 (2011).
- [5] E. Epelbaum, H. Krebs, and U. G. Meißner, Eur. Phys. J. A **51**, 53 (2015).
- [6] E. Epelbaum, H. Krebs, and U.-G. Meißner, Phys. Rev. Lett. **115**, 122301 (2015).
- [7] E. Epelbaum, W. Gloeckle, and U.-G. Meißner, Eur. Phys. J. A **19**, 125 (2004), arXiv:nucl-th/0304037.
- [8] E. Epelbaum, W. Gloeckle, and U.-G. Meißner, Eur. Phys. J. A **19**, 401 (2004), arXiv:nucl-th/0308010.
- [9] E. Epelbaum, W. Glockle, and U.-G. Meißner, Nucl. Phys. A **747**, 362 (2005).
- [10] E. Epelbaum, A. M. Gasparyan, J. Gegelia, and H. Krebs, Eur. Phys. J. A **51**, 71 (2015).
- [11] Y. Xiao, C.-X. Wang, J.-X. Lu, and L.-S. Geng, Phys. Rev. C **102**, 054001 (2020), arXiv:2007.13675 [nucl-th].
- [12] V. G. J. Stoks, R. A. M. Klomp, M. C. M. Rentmeester, and J. J. de Swart, Phys. Rev. C **48**, 792 (1993).
- [13] R. Machleidt, K. Holinde, and C. Elster, Phys. Rept. **149**, 1 (1987).
- [14] S. Shen, H. Liang, W. H. Long, J. Meng, and P. Ring, Prog. Part. Nucl. Phys. **109**, 103713 (2019), arXiv:1904.04977 [nucl-th].
- [15] R. Navarro Pérez, J. E. Amaro, and E. Ruiz Arriola, Phys.

- Rev. C **88**, 024002 (2013), [Erratum: Phys. Rev. C 88, 069902 (2013)], arXiv:1304.0895 [nucl-th].
- [16] R. Navarro Pérez, J. E. Amaro, and E. Ruiz Arriola, Phys. Rev. C **91**, 054002 (2015), arXiv:1411.1212 [nucl-th].
- [17] R. Navarro Pérez, J. E. Amaro, and E. Ruiz Arriola, Phys. Rev. C **95**, 064001 (2017), arXiv:1606.00592 [nucl-th].
- [18] A. G. Escalante, R. Navarro Pérez, and E. Ruiz Arriola, Phys. Rev. C **104**, 054002 (2021), arXiv:2010.03885 [nucl-th].
- [19] R. J. Furnstahl, N. Klco, D. R. Phillips, and S. Wesolowski, Phys. Rev. C **92**, 024005 (2015), arXiv:1506.01343 [nucl-th].
- [20] J. A. Melendez, S. Wesolowski, and R. J. Furnstahl, Phys. Rev. C **96**, 024003 (2017), arXiv:1704.03308 [nucl-th].
- [21] J. A. Melendez, R. J. Furnstahl, D. R. Phillips, M. T. Pratola, and S. Wesolowski, Phys. Rev. C **100**, 044001 (2019), arXiv:1904.10581 [nucl-th].
- [22] E. Epelbaum *et al.*, Eur. Phys. J. A **56**, 92 (2020), arXiv:1907.03608 [nucl-th].
- [23] E. Epelbaum, H. Krebs, and P. Reinert, Front. in Phys. **8**, 98 (2020), arXiv:1911.11875 [nucl-th].
- [24] P. Maris *et al.*, Phys. Rev. C **103**, 054001 (2021), arXiv:2012.12396 [nucl-th].